

A multi-temperature universe can allow a sub-MeV dark photon dark matter

Amin Aboubrahim,^{1,*} Wan-Zhe Feng,^{2,†} Pran Nath,^{3,‡} and Zhu-Yao Wang^{3,§}

¹*Institut für Theoretische Physik, Westfälische Wilhelms-Universität Münster,
Wilhelm-Klemm-Straße 9, 48149 Münster, Germany*

²*Center for Joint Quantum Studies and Department of Physics,
School of Science, Tianjin University, Tianjin 300350, P.R. China*

³*Department of Physics, Northeastern University, Boston, MA 02115-5000, USA*

(Dated: March 1, 2025)

An analysis of sub-MeV dark photon as dark matter is given which is achieved with two hidden sectors, one of which interacts directly with the visible sector while the second has only indirect coupling with the visible sector. The formalism for the evolution of three bath temperatures for the visible sector and the two hidden sectors is developed and utilized in solution of Boltzmann equations coupling the three sectors. We present exclusion plots where the sub-MeV dark photon can be dark matter. The analysis can be extended to a multi-temperature universe with multiple hidden sectors and multiple heat baths.

PACS numbers:

Introduction: Supergravity and strings models typically contain hidden sectors with gauge groups including $U(1)$ gauge group factors. These hidden sectors with $U(1)$ gauge groups can interact feebly with the visible sector and interact feebly or with normal strength with each other. The fields in the visible and hidden sectors in general will reside in different heat baths and the universe in this case will be a multi-temperature universe. The multi-temperature nature of the universe becomes a relevant issue if the observables in the visible sector are functions of the visible and the hidden sector heat baths. Such is the situation if dark matter (DM) resides in the hidden sector but interacts feebly with the visible sector. In this case an accurate computation of the relic density requires thermal averaging of cross sections and decay widths which depend on temperatures of both the visible and the hidden sector heat baths. In this Letter we develop a theoretical formalism which can correlate the evolution of temperatures of the hidden sector and of the visible sectors (for the specific case of two hidden sectors) in an accurate way.

The formalism noted above is used in the investigation of a dark photon and dark fermions of hidden sectors as possible DM candidates. There exists a considerable literature in the study of dark photons [1–14] (for review see [15–17]) to which the interested reader is directed. While axions and dark photons in the light to ultralight mass region (from keV to 10^{-22} eV) have been investigated [12, 14, 18–22], the sub-MeV dark photon mass range appears difficult to realize. The problem arises in part because with the visible sector interacting with a hidden sector via kinetic mixing, the twin constraints that the dark photon has a lifetime larger than the age of the universe, and also produce a sufficient amount of DM to populate the universe are difficult to satisfy

In this Letter we show that a sub-MeV dark photon as

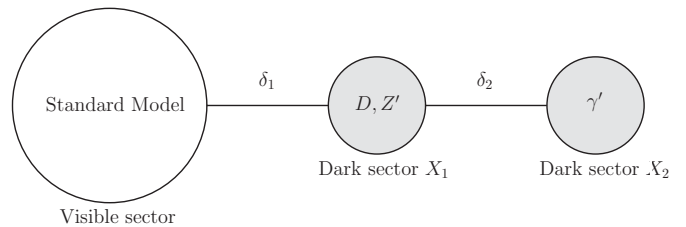


FIG. 1: The exhibition of the model we consider in the paper. The standard model has a direct coupling with hidden sector X_1 with strength proportional to δ_1 , whereas hidden sector X_2 only interacts directly with X_1 with strength proportional to δ_2 , and thus X_2 interacts with the standard model only indirectly.

DM can indeed be realized in a simple extension of the Standard Model (SM) where the hidden sector is constituted of two sectors X_1 and X_2 where the sector X_1 has kinetic mixing with the visible sector while the sector X_2 has kinetic and mass mixings only with sector X_1 , c.f., Fig. 1. We assume that the hidden sector X_1 has a dark fermion D and its gauge boson Z' decays before the BBN while the hidden sector X_2 has only a dark photon γ' which has a lifetime larger than the age of the Universe. This set up is theoretically more complex because here one has three heat baths and the computation of the relic density thus depends on three temperatures, i.e., the temperature T of the visible sector, the temperature T_1 of the hidden sector X_1 and the temperature T_2 of the hidden sector X_2 . In the following we develop a formalism that allows one to compute temperatures of all three heat baths in terms of one common temperature, which can be chosen to be T , T_1 or T_2 . In the analysis below it is found convenient to choose the reference temperature to be T_1 .

The model: As noted in the Introduction we consider an

extension of the SM with two dark sectors: X_1 and X_2 . We assume that the two sectors X_1 and X_2 have $U(1)_{X_1}$ and $U(1)_{X_2}$ gauge symmetries and that the field content of X_1 is (C_μ, D) where C_μ is the gauge field and D is a dark fermion, and the field content of X_2 is the gauge field D_μ and there is no dark fermion in the sector X_2 . We invoke a kinetic mixing [23, 24] between the hypercharge field B_μ of SM and C_μ and a kinetic mixing between C_μ and D_μ as well as a Stueckelberg mass growth [25–29] for all the gauge fields as well as a Stueckelberg mass mixing between the fields C_μ and D_μ . The extended part of the Lagrangian including both the kinetic and mass mixings in the unitary gauge is given by

$$\begin{aligned} \mathcal{L}_{\text{kin}} = & -\frac{1}{4}B^{\mu\nu}B_{\mu\nu} - \frac{1}{4}C^{\mu\nu}C_{\mu\nu} - \frac{1}{4}D^{\mu\nu}D_{\mu\nu} \\ & - \frac{\delta_1}{2}B^{\mu\nu}C_{\mu\nu} - \frac{\delta_2}{2}C^{\mu\nu}D_{\mu\nu} \\ & - \frac{1}{2}(M_1C_\mu + M_2B_\mu)^2 - \frac{1}{2}(M_3C_\mu + M_4D_\mu)^2. \end{aligned} \quad (1)$$

The D fermion is assumed charged under $U(1)_{X_1}$ with interaction $g_X \bar{D}\gamma^\mu DC_\mu$. The neutral current Lagrangian emerging from Eq. (1) for the mass eigenstates γ', Z', Z, γ describing the couplings between the vector bosons γ', Z', Z, γ with the visible sector fermions is given by

$$\begin{aligned} \mathcal{L}_{\text{NC}}^v = & \frac{g_2}{2\cos\theta_w} \bar{f}\gamma^\mu [(v_f - a_f\gamma_5)Z_\mu + (v'_f - a'_f\gamma_5)Z'_\mu \\ & + (v''_f - a''_f\gamma_5)A_\mu] f + e\bar{f}\gamma^\mu Q_f A_\mu f. \end{aligned} \quad (2)$$

Here θ_w is the weak angle and e is defined as

$$\frac{1}{e^2} = \frac{1}{g_2^2} + \frac{1 + \epsilon_1^2 - 2\epsilon_1\delta_1 + \epsilon_1^2\epsilon_2^2 - 2\epsilon_1^2\epsilon_2\delta_2}{g_Y^2}, \quad (3)$$

where $\epsilon_1 = M_2/M_1$ and $\epsilon_2 = M_3/M_4$. The neutral current Lagrangian for coupling to the hidden sector fermion is given by

$$\mathcal{L}_{\text{NC}}^h = (c_{\gamma'}A_\mu^{\gamma'} + c_Z Z_\mu + c_{Z'}Z'_\mu + c_\gamma A_\mu^\gamma)\bar{D}\gamma^\mu D, \quad (4)$$

where

$$c_{\gamma'} \simeq g_X \frac{m_{\gamma'}^2}{m_{Z'}^2 - m_{\gamma'}^2} \delta_2, \quad c_Z \simeq g_X \delta_1 \sin\theta_w (1 + \epsilon_z^2), \quad (5)$$

$$c_{Z'} \simeq g_X, \quad c_\gamma \simeq -g_X \delta_1 \delta_2 \left(\frac{m_{\gamma'}}{m_{Z'}} \right)^2 \sin\beta \cos\theta_w, \quad (6)$$

$$\tan 2\beta = \frac{2M_3M_4}{M_4^2 - M_1^2 - M_3^2}, \quad \epsilon_z = m_{Z'}/m_Z. \quad (7)$$

Boltzmann equations for yields with three bath temperatures: The relic densities of the dark photon and of the dark fermion arise in part from a freeze-in mechanism [30–34]. In general the visible sector and the dark sectors will have different temperatures [35–40] (a similar setup has been considered in Ref. [40] but with a

different particle content, couplings and no explicit multi-temperature evolution. Also the DM candidate was not the dark photon as in our case). As mentioned above, we consider three different temperatures corresponding to the temperatures of the visible sector T and of the two hidden sectors, T_1 for X_1 and T_2 for X_2 . Defining the yield $Y = n/s$, where n is the number density and s is the entropy density, and the bath functions η and ζ so that $T = \eta T_1$ and $T_2 = \zeta T_1$, we write the Boltzmann equations for the yields as

$$\begin{aligned} \frac{dY_D}{dT_1} = & -\frac{d\rho/dT_1}{4H\rho} s \left[\langle\sigma v\rangle_{i\bar{i}\rightarrow D\bar{D}}(\eta T_1) Y_i^2(\eta T_1) \right. \\ & - \frac{1}{2}\langle\sigma v\rangle_{D\bar{D}\rightarrow i\bar{i}}(T_1) Y_D^2 + \langle\sigma v\rangle_{Z'Z'\rightarrow D\bar{D}}(T_1) Y_{Z'}^2 \\ & - \frac{1}{2}\langle\sigma v\rangle_{D\bar{D}\rightarrow Z'Z'}(T_1) Y_D^2 - \frac{1}{2}\langle\sigma v\rangle_{D\bar{D}\rightarrow \gamma'\gamma'}(T_1) Y_D^2 \\ & + \langle\sigma v\rangle_{\gamma'\gamma'\rightarrow D\bar{D}}(\zeta T_1) Y_{\gamma'}^2 - \frac{1}{2}\langle\sigma v\rangle_{D\bar{D}\rightarrow Z'\gamma'}(T_1) Y_D^2 \\ & \left. + \langle\sigma v\rangle_{Z'\gamma'\rightarrow D\bar{D}}(T_1, \zeta T_1) Y_{Z'} Y_{\gamma'} \right], \end{aligned} \quad (8)$$

$$\begin{aligned} \frac{dY_{Z'}}{dT_1} = & -\frac{d\rho/dT_1}{4H\rho} s \left[\langle\sigma v\rangle_{i\bar{i}\rightarrow Z'Z'}(\eta T_1) Y_i^2(\eta T_1) \right. \\ & - \langle\sigma v\rangle_{Z'Z'\rightarrow i\bar{i}}(T_1) Y_{Z'}^2 - \langle\sigma v\rangle_{Z'Z'\rightarrow D\bar{D}}(T_1) Y_{Z'}^2 \\ & + \langle\sigma v\rangle_{i\bar{i}\rightarrow Z'}(\eta T_1) Y_i^2(\eta T_1) + \frac{1}{2}\langle\sigma v\rangle_{D\bar{D}\rightarrow Z'Z'}(T_1) Y_D^2 \\ & + \frac{1}{2}\langle\sigma v\rangle_{D\bar{D}\rightarrow Z'\gamma'}(T_1) Y_D^2 - \frac{1}{s}\langle\Gamma_{Z'\rightarrow i\bar{i}}\rangle(T_1) Y_{Z'} \\ & \left. - \langle\sigma v\rangle_{Z'\gamma'\rightarrow D\bar{D}}(T_1, \zeta T_1) Y_{Z'} Y_{\gamma'} \right], \end{aligned} \quad (9)$$

$$\begin{aligned} \frac{dY_{\gamma'}}{dT_1} = & -\frac{d\rho/dT_1}{4H\rho} s \left[\frac{1}{2}\langle\sigma v\rangle_{D\bar{D}\rightarrow \gamma'\gamma'}(T_1) Y_D^2 \right. \\ & - \langle\sigma v\rangle_{\gamma'\gamma'\rightarrow D\bar{D}}(\zeta T_1) Y_{\gamma'}^2 + \langle\sigma v\rangle_{i\bar{i}\rightarrow \gamma'}(\eta T_1) Y_i^2(\eta T_1) \\ & + \langle\sigma v\rangle_{i\bar{i}\rightarrow \gamma'\gamma'}(\eta T_1) Y_i^2(\eta T_1) - \langle\sigma v\rangle_{\gamma'\gamma'\rightarrow i\bar{i}}(\zeta T_1) Y_{\gamma'}^2 \\ & - \frac{1}{s}\langle\Gamma_{\gamma'\rightarrow i\bar{i}}\rangle(\zeta T_1) Y_{\gamma'} + \frac{1}{2}\langle\sigma v\rangle_{D\bar{D}\rightarrow Z'\gamma'}(T_1) Y_D^2 \\ & \left. - \langle\sigma v\rangle_{Z'\gamma'\rightarrow D\bar{D}}(T_1, \zeta T_1) Y_{Z'} Y_{\gamma'} \right], \end{aligned} \quad (10)$$

where H is the Hubble parameter and ρ is the energy density. Detailed formulae for the cross sections that enter in the yield equations are given in the Supplemental Material.

Evolution of bath temperatures of hidden and visible sectors: The yield equations involve computation of cross sections and decay widths at bath temperatures of the visible sector and the hidden sectors which are in general different. The ratio of the bath temperatures are encoded in the functions η and ζ and their evolution are

given below:

$$\frac{d\eta}{dT_1} = -\frac{\eta}{T_1} + \left(\frac{4H\rho_v + j_1 + j_2}{4H\rho_1 - j_1} \right) \frac{d\rho_1/dT_1}{T_1 \frac{d\rho_v}{dT}}, \quad (11)$$

$$\frac{d\zeta}{dT_1} = -\frac{\zeta}{T_1} + \left(\frac{4H\rho_2 - j_2}{4H\rho_1 - j_1} \right) \frac{d\rho_1/dT_1}{T_1 \frac{d\rho_2}{dT_2}}, \quad (12)$$

where

$$\frac{d\rho}{dT_1} = \left(\frac{4H\rho}{4H\rho_1 - j_1} \right) \frac{d\rho_1}{dT_1}, \quad \frac{d\rho_v}{dT} = \frac{\pi^2}{30} \left(\frac{dg_{\text{eff}}^v}{dT} \eta^4 T_1^4 + 4g_{\text{eff}}^v \eta^3 T_1^3 \right), \quad (13)$$

$$\frac{d\rho_1}{dT_1} = \frac{\pi^2}{30} \left(\frac{dg_{1\text{eff}}}{dT_1} T_1^4 + 4g_{1\text{eff}} T_1^3 \right), \quad \frac{d\rho_2}{dT_2} = \frac{\pi^2}{30} \left(\frac{dg_{2\text{eff}}}{dT_2} \zeta^4 T_1^4 + 4g_{2\text{eff}} \zeta^3 T_1^3 \right), \quad (14)$$

$$s = \frac{2\pi^2}{45} (h_{\text{eff}}^v T^3 + h_{1\text{eff}} T_1^3 + h_{2\text{eff}} T_2^3), \quad H^2 = \frac{8\pi G_N}{3} (\rho_v + \rho_1 + \rho_2). \quad (15)$$

The deduction of the evolution equations for η and ζ and for the effective entropy and energy degrees of freedom h_{eff} and g_{eff} are given in the Supplemental Material.

Dark photon lifetime: The partial decay width of γ' to two neutrinos is given by

$$\Gamma_{\gamma' \rightarrow \nu\bar{\nu}} = \frac{g_2^2 \delta_1^2 (\delta_2 - \sin \beta)^2 \epsilon_{\gamma'}^4}{8\pi} m_{\gamma'} \tan^2 \theta_w, \quad (16)$$

where $\epsilon_{\gamma'} = m_{\gamma'}/m_Z$, and the partial decay width of γ' to three photons reads [19, 41]

$$\Gamma_{\gamma' \rightarrow 3\gamma} = \frac{17\alpha^3 \alpha'}{2^7 3^6 5^3 \pi^3} \frac{m_{\gamma'}^9}{m_e^8} \approx 4.70 \times 10^{-8} \alpha^3 \alpha' \frac{m_{\gamma'}^9}{m_e^8}, \quad (17)$$

where $\alpha = e^2/4\pi$, $\alpha' = (ke)^2/4\pi$ and $k = -\delta_1(\delta_2 - \sin \beta) \cos \theta_w$.

Numerical analysis: In the analysis we make certain that the relic density of the dark relics is consistent with the Planck data. Contribution to the relic density arise from γ' and D while Z' decays before BBN and is removed from the spectrum. In Table I we present four benchmarks which satisfy all the experimental constraints. The relic density shown is that of γ' while that of D is only $\mathcal{O}(10^{-6})$ or less and thus negligible. The dark photon is long lived with a lifetime larger than the age of the universe. As an illustration the model point (d) gives $\tau_{\gamma' \rightarrow \nu\bar{\nu}} \sim 8.4 \times 10^{21}$ yrs and $\tau_{\gamma' \rightarrow 3\gamma} \sim 5.3 \times 10^{15}$ yrs.

Calculation of the relic density requires determining the yields by numerically solving the five stiff coupled equations, Eqs. (8)–(12). The resulting yields for D , Z' and γ' as a function of the hidden sector temperature T_1 are shown in Fig. 2 for benchmarks (a) and (b). As the universe cools, the number densities of D , Z' and γ' increase gradually. At around $T_1 = 100$ GeV, the dark fermions D start to freeze-out, and the blue curve becomes flat around $T_1 = 0.1$ GeV. After the dark fermion

decouples, the dynamics of Z' and γ' is affected mainly by SM particles freeze-in processes after $T_1 = 0.1$ GeV. However, since Z' is unstable its density depletes to zero at $T_1 \sim 10^{-4}$ GeV. The only particles that contribute to the relic density then are D (blue curve) and γ' (yellow curve). As noted the analysis gives dark photon as the dominant component of DM.

Thermalization and dark freeze-out: The upper panel of Fig. 3 gives the evolution of $\xi = T_1/T$ as a function of T_1 which shows that ξ rises until it thermalizes with the visible sector, i.e., $\xi \sim 1$. The middle panel of this figure gives the evolution $\zeta = T_2/T_1$ as a function of T_1 while the bottom panel of Fig. 3 gives the evolution of $\kappa = T_2/T$ as function of T . We note that X_2 does not thermalize with X_1 . This happens because the energy injection from X_1 into X_2 is not efficient enough. Consequently $T_2/T \ll 1$ which also has implications for ΔN_{eff} as we explain later. In Fig. 4 we show $n\langle\sigma v\rangle$ and the thermally averaged Z' decay width as a function of T_1 for benchmark (a). Also shown is the Hubble parameter $H(T_1)$. As evident, while Z' can enter into equilibrium with the visible sector for a period of time, the dark photon barely does so. We indicate by arrows the point at which the dark freeze-out of D and γ' occurs. The dark photons decouple earlier followed by the dark fermions which is also evident in Fig. 2. We note that $\langle\Gamma_{Z'}\rangle$ overtakes $H(T_1)$ at lower temperatures contributing to the depletion of Z' number density.

We note that the parameter space of Z' and γ' is constrained by experiments such as BaBar, CHARM and other beam-dump experiments as well as by astrophysical data from Supernova SN1987A and stellar cooling. Those limits become even stronger when the dark photon is assumed to be the DM particle. Thus, measurements of heating rates of the Galactic center cold gas clouds [42], the temperature of the diffuse X-ray background [43] as

TABLE I: Benchmarks used in this analysis where $g_X = 0.95$ and masses are in MeV except m_D which is in GeV.

Model	m_D	M_1	M_3	M_4	δ_1	δ_2	$m_{Z'}$	$m_{\gamma'}$	Ωh^2
(a)	1.00	4.50	0.0	0.43	4.0×10^{-10}	0.40	4.90	0.43	0.124
(b)	0.50	4.50	0.0	0.47	6.5×10^{-11}	0.40	4.90	0.47	0.103
(c)	0.05	4.50	0.0	0.45	5.6×10^{-12}	0.40	4.91	0.45	0.102
(d)	0.62	4.50	-5.0	0.45	4.0×10^{-10}	0.05	6.76	0.30	0.108

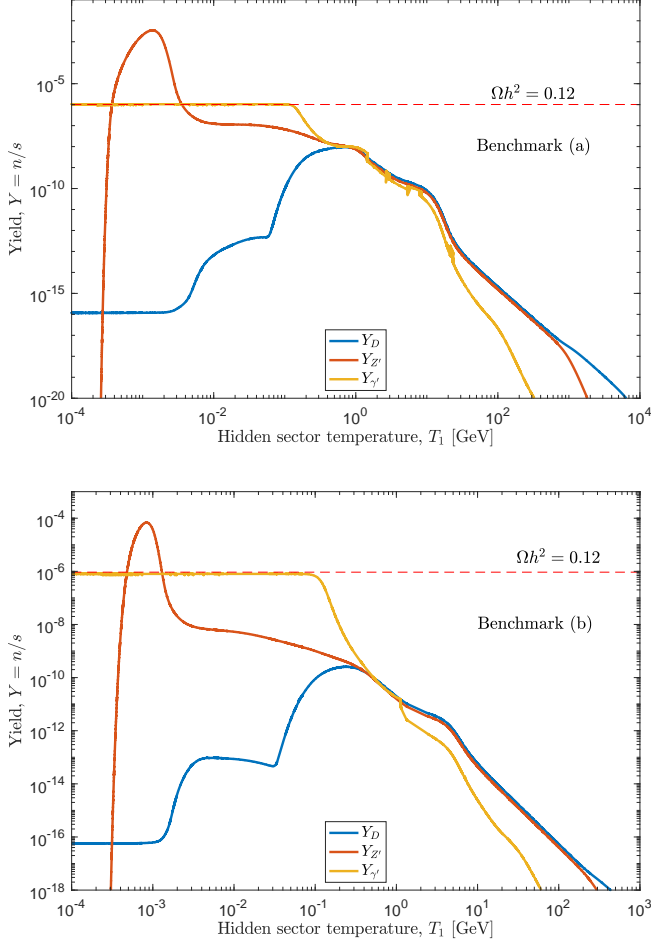


FIG. 2: The yields for the dark fermion D and the dark bosons Z' and γ' as a function of the hidden sector temperature T_1 for benchmarks (a) (upper panel) and (b) (bottom panel). The horizontal dashed line corresponds to the observed relic density which matches the freeze-out yield of γ' . Note that at dark freeze-out $Y_D \ll Y_{\gamma'}$.

well as that of the intergalactic medium at the time of He^{++} reionization [44–46] are affected by early $\gamma' \rightarrow 3\gamma$ decays. Further constraints can be derived from energy injection during the dark ages [47] and spectral distortion of the CMB [46]. The presence of a long-lived sub-MeV particle species can contribute to the relativistic number of degrees of freedom ΔN_{eff} during BBN and recombination [48]. The recast limits from all these ex-

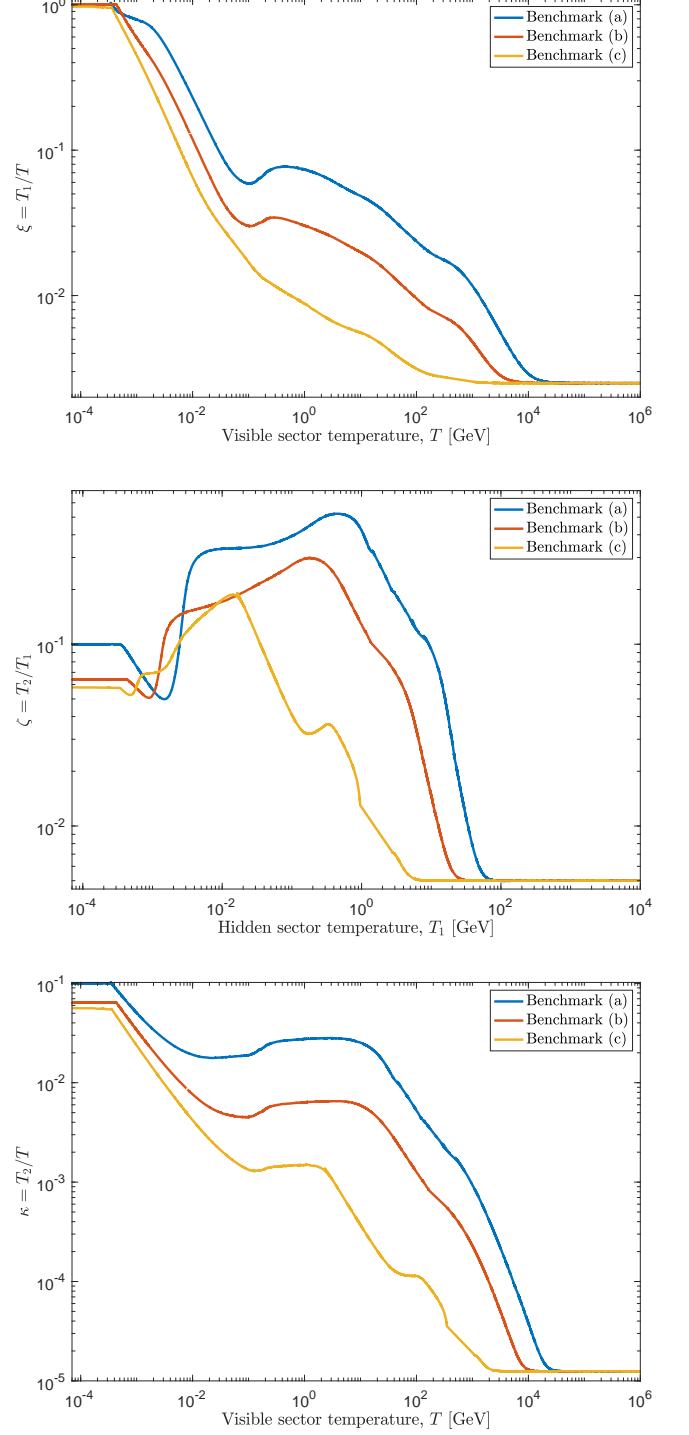


FIG. 3: Evolution of ξ (upper panel) and κ (bottom panel) as a function of the visible sector temperature T and that of ζ (middle panel) as a function of T_1 for three benchmarks (a), (b) and (c) of Table I.

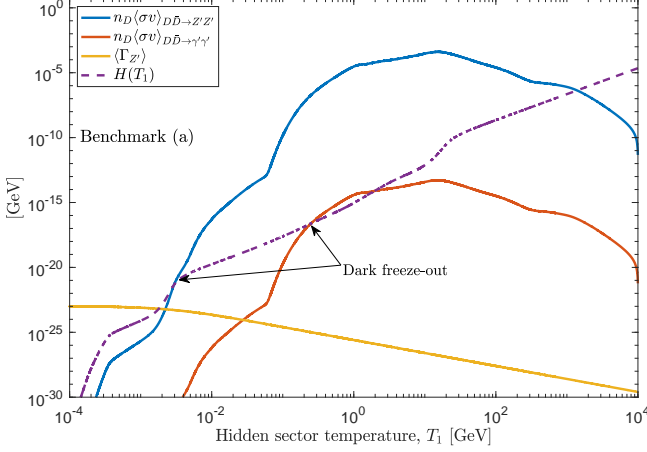


FIG. 4: A plot of $n\langle\sigma v\rangle$ for the dominant processes in the hidden sector along with the Hubble parameter and the thermally averaged decay width of Z' .

periments are summarized in Fig. 5. In our model, the limits on dark photon DM are relaxed due to its doubly suppressed coupling with the SM which is proportional to $\delta_1(\delta_2 - \sin\beta)$. A reduced parameter space for Z' and γ' is still allowed. A scan of the parameter space within this allowed region results in a set of models with the correct relic density. Assuming a 2σ band, we exhibit the allowed parameter space where the dark photon is a viable DM candidate. This is indicated in Fig. 5 by “freeze-in”. The different shades of blue correspond to different choices of m_D . In each panel, we fix g_X and δ_2 and scan over δ_1 and $m_{\gamma'}$ with different choices of m_D . Due to the negligible number of D fermions, g_X is not constrained by Planck experiment [49, 50] in the channel $D\bar{D} \rightarrow Z'Z' \rightarrow 4e$. This allows the process $D\bar{D} \rightarrow \gamma'\gamma'$ to be the dominant production mechanism of γ' . Alternate production mechanisms for the dark photon have been alluded to in Ref. [43] as a possible way to generate a dark photon DM which is exactly what our model does.

Finally, we check the number of relativistic degrees of freedom generated by the dark photon at BBN time. The SM gives $N_{\text{eff}} = 3.046$. The dark photon contribution is given by

$$\Delta N_{\text{eff}} \simeq \frac{12}{7} \left(\frac{11}{4} \right)^{\frac{4}{3}} \left(\frac{T_2}{T_\gamma} \right)^4, \quad (18)$$

where $T_\gamma = T$. Using the ratio of the temperatures $T_2/T < 0.1$ from Fig. 3, one finds that ΔN_{eff} is $\mathcal{O}(10^{-4})$ which makes a negligible contribution to the SM N_{eff} .

Conclusion: In this work we discussed the possibility that DM in the universe is constituted of sub-MeV dark photons which reside in the hidden sector. In this case a proper analysis of the relic density requires a solution to coupled Boltzmann equations which depend on multiple bath temperatures including the bath temperature

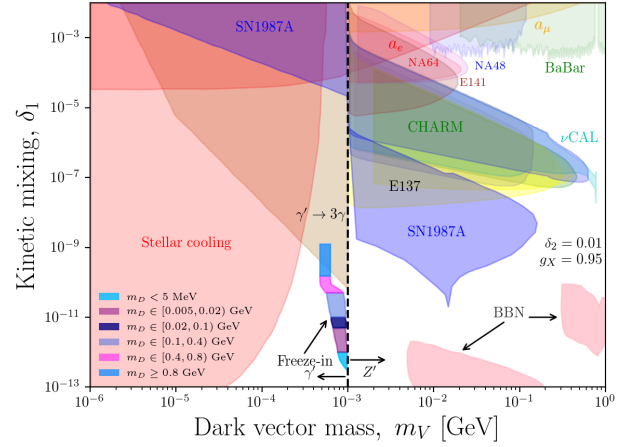
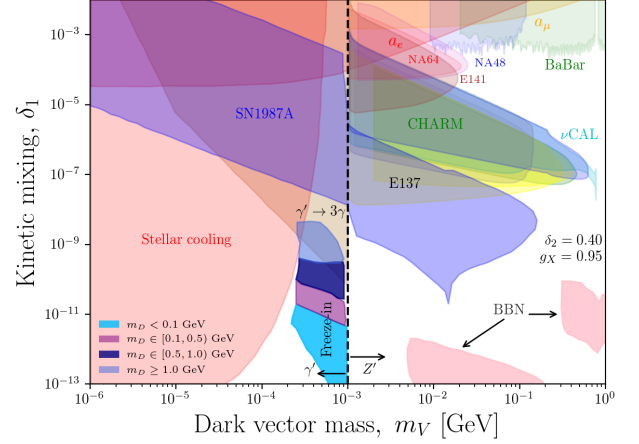


FIG. 5: Exclusion limits from terrestrial and astrophysical experiments on dark photon which has kinetic mixings with the SM sector. Excluded regions are due to constraints from experiments which include electron and muon $g - 2$ [51], BaBar [52], CHARM [53, 54], NA48 [55], E137 [56, 57], NA64 [58, 59], E141 [60] and ν -CAL [54, 61, 62]. The limits are obtained from `darkcast` [63]. The strongest constraints on a dark photon (mass less than 1 MeV) come from Supernova SN1987A (including a robustly excluded region and systematic uncertainties) [64], stellar cooling [65] and from decay to 3γ on cosmological timescales [43, 66]. The islands in pink are constraints from BBN. The region where the freeze-in relic density is satisfied within 2σ of the experimental constraint is shown in different shades of blue corresponding to different choices of m_D . In the upper panel, $m_{Z'} = (5 - 20)m_{\gamma'}$ and $\delta_2 = 0.4$ while in the lower panel $m_{Z'} = 3$ MeV and $\delta_2 = 0.01$.

for the visible sector and those for all the hidden sectors that are feebly coupled with the visible sector. In this Letter we discussed a model where the visible sector couples with two hidden sectors X_1 and X_2 and where the particles in the hidden sector consist of a dark fermion, a dark Z' and a dark photon. The dark Z' decays and disappears from the spectrum while the dark photon is a long lived relic. We show that the relic density of the

dark photon depends critically on temperatures of both the visible and the hidden sectors. We present exclusion plots where a sub-MeV dark photon can exist consistent with all the current experimental constraints. We also show that the existence of a dark photon is consistent with the constraints on N_{eff} from BBN. Thus a sub-MeV dark photon is a viable candidate for DM within a constrained parameter space of mass and kinetic couplings. The formalism developed here of correlated evolution of bath temperatures in the visible and hidden sectors may find application for a wider class of phenomena involving hidden sectors.

The research of AA was supported by the BMBF under contract 05H18PMCC1. The research of WZF was supported in part by the National Natural Science Foundation of China under Grant No. 11905158 and No. 11935009. The research of PN and ZYW was supported in part by the NSF Grant PHY-191332.

* Email: aabouibr@uni-muenster.de; ORCID: 0000-0002-1110-4265

† Email: vicf@tju.edu.cn; ORCID: 0000-0003-2488-0041

‡ Email: p.nath@northeastern.edu; ORCID: 0000-0001-9879-9751

§ Email: wang.zhu@northeastern.edu; ORCID: 0000-0001-5398-7302

- [1] M. R. Buckley and P. J. Fox, Phys. Rev. D **81**, 083522 (2010) doi:10.1103/PhysRevD.81.083522 [arXiv:0911.3898 [hep-ph]].
- [2] A. Loeb and N. Weiner, Phys. Rev. Lett. **106**, 171302 (2011) doi:10.1103/PhysRevLett.106.171302 [arXiv:1011.6374 [astro-ph.CO]].
- [3] M. Kaplinghat, S. Tulin and H. B. Yu, Phys. Rev. Lett. **116**, no.4, 041302 (2016) doi:10.1103/PhysRevLett.116.041302 [arXiv:1508.03339 [astro-ph.CO]].
- [4] L. Sagunski, S. Gad-Nasr, B. Colquhoun, A. Robertson and S. Tulin, JCAP **01**, 024 (2021) doi:10.1088/1475-7516/2021/01/024 [arXiv:2006.12515 [astro-ph.CO]].
- [5] A. Aboubrahim, W. Z. Feng, P. Nath and Z. Y. Wang, [arXiv:2008.00529 [hep-ph]] (to appear in PRD).
- [6] P. W. Graham, J. Mardon and S. Rajendran, Phys. Rev. D **93**, no.10, 103520 (2016) doi:10.1103/PhysRevD.93.103520 [arXiv:1504.02102 [hep-ph]].
- [7] K. Kaneta, H. S. Lee and S. Yun, Phys. Rev. Lett. **118**, no.10, 101802 (2017) doi:10.1103/PhysRevLett.118.101802 [arXiv:1611.01466 [hep-ph]].
- [8] K. Kaneta, H. S. Lee and S. Yun, Phys. Rev. D **95**, no.11, 115032 (2017) doi:10.1103/PhysRevD.95.115032 [arXiv:1704.07542 [hep-ph]].
- [9] R. T. Co, A. Pierce, Z. Zhang and Y. Zhao, Phys. Rev. D **99**, no.7, 075002 (2019) doi:10.1103/PhysRevD.99.075002 [arXiv:1810.07196 [hep-ph]].
- [10] J. A. Dror, K. Harigaya and V. Narayan, Phys. Rev. D **99**, no.3, 035036 (2019) doi:10.1103/PhysRevD.99.035036 [arXiv:1810.07195 [hep-ph]].
- [11] P. Agrawal, N. Kitajima, M. Reece, T. Sekiguchi and F. Takahashi, Phys. Lett. B **801**, 135136 (2020) doi:10.1016/j.physletb.2019.135136 [arXiv:1810.07188 [hep-ph]].
- [12] A. J. Long and L. T. Wang, Phys. Rev. D **99**, no.6, 063529 (2019) doi:10.1103/PhysRevD.99.063529 [arXiv:1901.03312 [hep-ph]].
- [13] G. Alonso-Álvarez, T. Hugle and J. Jaeckel, JCAP **02**, 014 (2020) doi:10.1088/1475-7516/2020/02/014 [arXiv:1905.09836 [hep-ph]].
- [14] Y. Nakai, R. Namba and Z. Wang, JHEP **12**, 170 (2020) doi:10.1007/JHEP12(2020)170 [arXiv:2004.10743 [hep-ph]].
- [15] S. Tulin and H. B. Yu, Phys. Rept. **730**, 1-57 (2018) doi:10.1016/j.physrep.2017.11.004 [arXiv:1705.02358 [hep-ph]].
- [16] J. Alexander, M. Battaglieri, B. Echenard, R. Essig, M. Graham, E. Izaguirre, J. Jaros, G. Krnjaic, J. Mardon and D. Morrissey, *et al.* [arXiv:1608.08632 [hep-ph]].
- [17] M. Fabbrichesi, E. Gabrielli and G. Lanfranchi, doi:10.1007/978-3-030-62519-1 [arXiv:2005.01515 [hep-ph]].
- [18] I. M. Bloch, R. Essig, K. Tobioka, T. Volansky and T. T. Yu, JHEP **06**, 087 (2017) doi:10.1007/JHEP06(2017)087 [arXiv:1608.02123 [hep-ph]].
- [19] M. Pospelov, A. Ritz and M. B. Voloshin, Phys. Rev. D **78**, 115012 (2008) doi:10.1103/PhysRevD.78.115012 [arXiv:0807.3279 [hep-ph]].
- [20] J. E. Kim and D. J. E. Marsh, Phys. Rev. D **93**, no.2, 025027 (2016) doi:10.1103/PhysRevD.93.025027 [arXiv:1510.01701 [hep-ph]].
- [21] L. Hui, J. P. Ostriker, S. Tremaine and E. Witten, Phys. Rev. D **95**, no.4, 043541 (2017) doi:10.1103/PhysRevD.95.043541 [arXiv:1610.08297 [astro-ph.CO]].
- [22] J. Halverson, C. Long and P. Nath, Phys. Rev. D **96**, no.5, 056025 (2017) doi:10.1103/PhysRevD.96.056025 [arXiv:1703.07779 [hep-ph]].
- [23] B. Holdom, Phys. Lett. B **166**, 196-198 (1986) doi:10.1016/0370-2693(86)91377-8
- [24] M. Dutra, M. Lindner, S. Profumo, F. S. Queiroz, W. Rodejohann and C. Siqueira, JCAP **03**, 037 (2018) doi:10.1088/1475-7516/2018/03/037 [arXiv:1801.05447 [hep-ph]].
- [25] B. Kors and P. Nath, Phys. Lett. B **586**, 366-372 (2004) doi:10.1016/j.physletb.2004.02.051 [arXiv:hep-ph/0402047 [hep-ph]].
- [26] K. Cheung and T. C. Yuan, JHEP **03**, 120 (2007) doi:10.1088/1126-6708/2007/03/120 [arXiv:hep-ph/0701107 [hep-ph]].
- [27] D. Feldman, Z. Liu and P. Nath, JHEP **11**, 007 (2006) doi:10.1088/1126-6708/2006/11/007 [arXiv:hep-ph/0606294 [hep-ph]].
- [28] D. Feldman, Z. Liu and P. Nath, Phys. Rev. D **75**, 115001 (2007) doi:10.1103/PhysRevD.75.115001 [arXiv:hep-ph/0702123 [hep-ph]].
- [29] A. Aboubrahim and P. Nath, Phys. Rev. D **99**, no.5, 055037 (2019) doi:10.1103/PhysRevD.99.055037 [arXiv:1902.05538 [hep-ph]].
- [30] L. J. Hall, K. Jedamzik, J. March-Russell and S. M. West,

- JHEP **03**, 080 (2010) doi:10.1007/JHEP03(2010)080 [arXiv:0911.1120 [hep-ph]].
- [31] A. Aboubrahim, W. Z. Feng and P. Nath, JHEP **02**, 118 (2020) doi:10.1007/JHEP02(2020)118 [arXiv:1910.14092 [hep-ph]].
- [32] A. Aboubrahim, W. Z. Feng and P. Nath, JHEP **04**, 144 (2020) doi:10.1007/JHEP04(2020)144 [arXiv:2003.02267 [hep-ph]].
- [33] S. Koren and R. McGehee, Phys. Rev. D **101**, no.5, 055024 (2020) doi:10.1103/PhysRevD.101.055024 [arXiv:1908.03559 [hep-ph]].
- [34] Y. Du, F. Huang, H. L. Li and J. H. Yu, JHEP **12**, 207 (2020) doi:10.1007/JHEP12(2020)207 [arXiv:2005.01717 [hep-ph]].
- [35] J. L. Feng, H. Tu and H. B. Yu, JCAP **10**, 043 (2008) doi:10.1088/1475-7516/2008/10/043 [arXiv:0808.2318 [hep-ph]].
- [36] X. Chu, T. Hambye and M. H. G. Tytgat, JCAP **05**, 034 (2012) doi:10.1088/1475-7516/2012/05/034 [arXiv:1112.0493 [hep-ph]].
- [37] L. Ackerman, M. R. Buckley, S. M. Carroll and M. Kamionkowski, doi:10.1103/PhysRevD.79.023519 [arXiv:0810.5126 [hep-ph]].
- [38] R. Foot and S. Vagnozzi, Phys. Rev. D **91**, 023512 (2015) doi:10.1103/PhysRevD.91.023512 [arXiv:1409.7174 [hep-ph]].
- [39] R. Foot and S. Vagnozzi, JCAP **07**, 013 (2016) doi:10.1088/1475-7516/2016/07/013 [arXiv:1602.02467 [astro-ph.CO]].
- [40] T. Hambye, M. H. G. Tytgat, J. Vandecasteele and L. Vanderheyden, Phys. Rev. D **100**, no.9, 095018 (2019) doi:10.1103/PhysRevD.100.095018 [arXiv:1908.09864 [hep-ph]].
- [41] S. D. McDermott, H. H. Patel and H. Ramanani, Phys. Rev. D **97**, no.7, 073005 (2018) doi:10.1103/PhysRevD.97.073005 [arXiv:1705.00619 [hep-ph]].
- [42] A. Bhoonah, J. Bramante, F. Elahi and S. Schon, Phys. Rev. D **100**, no.2, 023001 (2019) doi:10.1103/PhysRevD.100.023001 [arXiv:1812.10919 [hep-ph]].
- [43] J. Redondo and M. Postma, JCAP **02**, 005 (2009) doi:10.1088/1475-7516/2009/02/005 [arXiv:0811.0326 [hep-ph]].
- [44] A. Caputo, H. Liu, S. Mishra-Sharma and J. T. Ruderman, Phys. Rev. Lett. **125**, no.22, 221303 (2020) doi:10.1103/PhysRevLett.125.221303 [arXiv:2002.05165 [astro-ph.CO]].
- [45] A. A. Garcia, K. Bondarenko, S. Ploekinger, J. Pradler and A. Sokolenko, JCAP **10**, 011 (2020) doi:10.1088/1475-7516/2020/10/011 [arXiv:2003.10465 [astro-ph.CO]].
- [46] S. J. Witte, S. Rosauro-Alcaraz, S. D. McDermott and V. Poulin, JHEP **06**, 132 (2020) doi:10.1007/JHEP06(2020)132 [arXiv:2003.13698 [astro-ph.CO]].
- [47] S. D. McDermott and S. J. Witte, Phys. Rev. D **101**, no.6, 063030 (2020) doi:10.1103/PhysRevD.101.063030 [arXiv:1911.05086 [hep-ph]].
- [48] P. Arias, D. Cadamuro, M. Goodsell, J. Jaeckel, J. Redondo and A. Ringwald, JCAP **06**, 013 (2012) doi:10.1088/1475-7516/2012/06/013 [arXiv:1201.5902 [hep-ph]].
- [49] P. A. R. Ade *et al.* [Planck], Astron. Astro-phys. **594**, A13 (2016) doi:10.1051/0004-6361/201525830 [arXiv:1502.01589 [astro-ph.CO]].
- [50] T. R. Slatyer, Phys. Rev. D **93**, no.2, 023527 (2016) doi:10.1103/PhysRevD.93.023527 [arXiv:1506.03811 [hep-ph]].
- [51] M. Endo, K. Hamaguchi and G. Mishima, Phys. Rev. D **86**, 095029 (2012) doi:10.1103/PhysRevD.86.095029 [arXiv:1209.2558 [hep-ph]].
- [52] J. P. Lees *et al.* [BaBar], Phys. Rev. Lett. **113**, no.20, 201801 (2014) doi:10.1103/PhysRevLett.113.201801 [arXiv:1406.2980 [hep-ex]].
- [53] F. Bergsma *et al.* [CHARM], Phys. Lett. B **157**, 458-462 (1985) doi:10.1016/0370-2693(85)90400-9
- [54] Y. D. Tsai, P. deNiverville and M. X. Liu, [arXiv:1908.07525 [hep-ph]].
- [55] J. R. Batley *et al.* [NA48/2], Phys. Lett. B **746**, 178-185 (2015) doi:10.1016/j.physletb.2015.04.068 [arXiv:1504.00607 [hep-ex]].
- [56] S. Andreas, C. Niebuhr and A. Ringwald, Phys. Rev. D **86**, 095019 (2012) doi:10.1103/PhysRevD.86.095019 [arXiv:1209.6083 [hep-ph]].
- [57] J. D. Bjorken, R. Essig, P. Schuster and N. Toro, Phys. Rev. D **80**, 075018 (2009) doi:10.1103/PhysRevD.80.075018 [arXiv:0906.0580 [hep-ph]].
- [58] D. Banerjee *et al.* [NA64], Phys. Rev. Lett. **120**, no.23, 231802 (2018) doi:10.1103/PhysRevLett.120.231802 [arXiv:1803.07748 [hep-ex]].
- [59] D. Banerjee *et al.* [NA64], Phys. Rev. D **101**, no.7, 071101 (2020) doi:10.1103/PhysRevD.101.071101 [arXiv:1912.11389 [hep-ex]].
- [60] E. M. Riordan, M. W. Krasny, K. Lang, P. De Barbaro, A. Bodek, S. Dasu, N. Varelas, X. Wang, R. G. Arnold and D. Benton, *et al.* Phys. Rev. Lett. **59**, 755 (1987) doi:10.1103/PhysRevLett.59.755
- [61] J. Blumlein, J. Brunner, H. J. Grabosch, P. Lanius, S. Nowak, C. Rethfeldt, H. E. Ryseck, M. Walter, D. Kiss and Z. Jaki, *et al.* Z. Phys. C **51**, 341-350 (1991) doi:10.1007/BF01548556
- [62] J. Blumlein, J. Brunner, H. J. Grabosch, P. Lanius, S. Nowak, C. Rethfeldt, H. E. Ryseck, M. Walter, D. Kiss and Z. Jaki, *et al.* Int. J. Mod. Phys. A **7**, 3835-3850 (1992) doi:10.1142/S0217751X9200171X
- [63] P. Ilten, Y. Soreq, M. Williams and W. Xue, JHEP **06**, 004 (2018) doi:10.1007/JHEP06(2018)004 [arXiv:1801.04847 [hep-ph]].
- [64] J. H. Chang, R. Essig and S. D. McDermott, JHEP **01**, 107 (2017) doi:10.1007/JHEP01(2017)107 [arXiv:1611.03864 [hep-ph]].
- [65] H. An, M. Pospelov and J. Pradler, Phys. Lett. B **725**, 190-195 (2013) doi:10.1016/j.physletb.2013.07.008 [arXiv:1302.3884 [hep-ph]].
- [66] R. Essig, E. Kuflik, S. D. McDermott, T. Volansky and K. M. Zurek, JHEP **11**, 193 (2013) doi:10.1007/JHEP11(2013)193 [arXiv:1309.4091 [hep-ph]].

A multi-temperature universe can allow a sub-MeV dark photon dark matter

Supplemental Material

Amin Aboubrabim, Wan-Zhe Feng, Pran Nath, and Zhu-Yao Wang

MULTI-TEMPERATURE UNIVERSE

As mentioned in the Letter, supergravity and string models contain hidden sectors. These hidden sectors in general would have both abelian and non-abelian gauge groups and some of them could interact feebly with the visible sector while others may interact with each other as shown in Fig. S1. Thus, for example, in D-brane models one gets $U(N)$ gauge groups where $U(N) \rightarrow SU(N) \times U(1)$. These extra $U(1)$ factors in general can acquire kinetic mixing with the $U(1)_Y$ of the visible sector. Further, the gauge bosons of the extra $U(1)$'s can acquire mass via the Stueckelberg mechanism and also have Stueckelberg mass mixings with the hypercharge gauge boson. Additionally if there are several hidden sector $U(1)$'s they can have also gauge and Stueckelberg mass mixings among themselves. Interestingly, the possible existence of these hidden sectors can have significant effect on model building in the visible sector. As an example one phenomenon which is deeply affected by the existence of hidden sectors is dark matter which we discuss in further detail below.

In general the dark sectors with a gauge symmetry will contain gauge fields as well as matter, but, as noted, typically they will have feeble interactions with the SM particles and likely also with the inflaton. This means that these particles would not be thermally produced in the reheat period after inflation but would then acquire their relic density via annihilation and decay of the SM particles. Thus in general the temperatures of the visible and the hidden sectors will be different from the visible sector as well as from each other. This means that their relic densities will be governed by a set of coupled Boltzmann equations which depend on different temperatures, i.e., temperature of the visible sector and those for the hidden sectors. One of the central items in understanding of how to deal with such coupled systems with sectors involving different temperatures is to understand fully how the temperatures of the hidden sectors grow relative to the visible sector temperature. The formalism of how to correlate the hidden and the visible sector temperatures was worked out for the case of the visible sector interacting with one hidden sector in [5]. However, a general framework does not exist. Here we discuss the case where there are two hidden sectors X_1 and X_2 where the hidden sector X_1 interacts with the visible sector, while the hidden sector X_2 interacts only with the hidden sector X_1 as shown in Fig. 1. In this case two functions $\eta^{-1} = \xi = T_1/T$ and $\zeta = T_2/T_1$ enter in the coupled Boltzmann equations and we derive differential equations for their evolution. The above setup has a direct application in achieving a sub-MeV dark photon as dark matter as explained in the Letter. However, a consistent analysis of the coupled dynamics of the visible sector and two hidden sectors is significantly more complex, and this Supplemental Material gives further details and derivations of many of the relations used in the Letter. The formalism developed here can be extended to multiple hidden sectors.

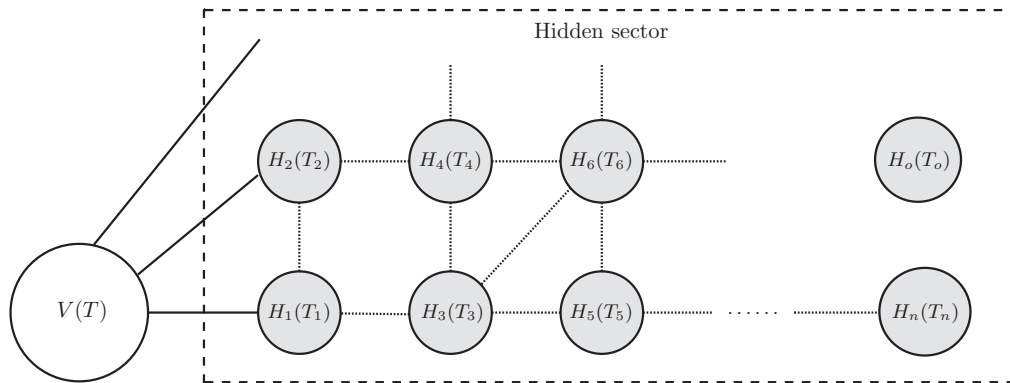


FIG. S1: A schematic diagram exhibiting the coupling of the visible sector with multiple dark sectors and of the dark sectors among themselves. The visible sector may have direct couplings with some of the dark sectors, or indirect couplings with others via interactions among the entire hidden sector.

CANONICAL NORMALIZATION OF EXTENDED $G_{SM} \times U(1)_{X_1} \times U(1)_{X_2}$ LAGRANGIAN WITH KINETIC AND STUECKELBERG MASS MIXINGS

Consider the Lagrangian

$$\mathcal{L} = -\frac{1}{4}V_{\mu\nu}^T K_E V^{\mu\nu} - \frac{1}{2}V^T M^2 V, \quad (S1)$$

where $V = (V_1, V_2, V_3, V_4)^T$ which we choose to be (D, C, B, A_3) . This Lagrangian can be put in the canonical form by appropriate transformations on K_E and M^2 . For the case when there is one dark sector it was done analytically in [28] and the basic reason which allows that to happen is that one of the eigenvalues of M^2 is zero corresponding to the photon which effectively reduces the analysis to two massive modes which can be handled analytically. In the present case since we have two hidden sectors, we have a 4×4 matrix, and while one of the eigenvalues corresponding to the photon is zero, one still has to deal with a cubic equation which, although possible to solve analytically, quickly becomes intractable in the presence of both kinetic and Stueckelberg mass mixing. However, because the kinetic mixings are typically small, it is possible to get accurate results by expanding couplings of the dark particles with the SM particles in powers of the kinetic mixings. In this case the relevant couplings can be recovered easily. However, such an expansion must occur around stable minima. This means that we must first diagonalize the SM mass squared matrix for the gauge bosons, and compute the kinetic mixing in this basis. We can then put the kinetic term in the canonical form. This step requires several $GL(2, \mathbb{R})$ transformations because of several mixings of the hidden sector with the visible sector and the mixing of the two hidden sectors. After the kinetic energy is put in the canonical form, we must write the mass square matrix of the gauge bosons in the same basis which then undiagonalizes the said matrix. However, because of the smallness of the kinetic mixings, we can carry out a perturbation expansion of the mass square matrix where the zeroth order mass square matrix is diagonal and the perturbations are proportional to the kinetic mixings and are small. We make this analysis concrete in the formalism below.

Let us consider an orthogonal transformation $V = RV^{(1)}$ such that $R^T M^2 R = M_D^2$ where M_D^2 is a diagonal matrix. In the $V^{(1)}$ basis the kinetic energy has the form $K'_E = R^T K_E R$. Next, let us make a transformation K such that $V^{(1)} = KV^{(n)}$, which could be a product of several sub-transformations, such that the kinetic energy is in the canonical form, i.e.,

$$K^T K'_E K = \mathbb{1}. \quad (S2)$$

In our case we will have $n = 8$ (as discussed below). In the $V^{(8)}$ basis, while the kinetic energy is in the canonical form, the mass matrix $M^2 = K^T M_D^2 K$ is not. However, as explained above since the kinetic mixings are small we can expand M^2 around $\delta_1 = 0 = \delta_2$ so that

$$K^T M_D^2 K = M_D^2 + \Delta M^2. \quad (S3)$$

Now since the kinetic mixing is supposed to be small, K differs from a unit matrix only by a small amount and thus ΔM^2 is small relative to M_D^2 and one may carry out perturbation expansion in ΔM^2 to arrive at the kinetic and mass mixing effects in the physical processes. To compute ΔM^2 we need K defined by Eq. (S2). The computation of K is significantly more complicated than for the case of one hidden sector. Below we give its computation in some detail.

While the procedure outlined above is general we will discuss the specific case where M^2 is block diagonal so that

$$M^2 = \begin{pmatrix} M_4^2 & M_3 M_4 & 0 & 0 \\ M_3 M_4 & M_3^2 + M_1^2 & 0 & 0 \\ 0 & 0 & \frac{1}{4}g_Y^2 v^2 & -\frac{1}{4}g_Y g_2 v^2 \\ 0 & 0 & -\frac{1}{4}g_Y g_2 v^2 & \frac{1}{4}g_2^2 v^2 \end{pmatrix}, \quad (S4)$$

where the upper right 2×2 matrix is for the hidden sector and the lower left 2×2 matrix is for the case of the standard model in the basis $V^T = (D_\mu, C_\mu, B_\mu, A_{3\mu})$. M^2 can be diagonalized by R where

$$R = \begin{pmatrix} R_\beta & 0 \\ 0 & R_w \end{pmatrix}, \quad R_\beta = \begin{pmatrix} \cos \beta & -\sin \beta \\ \sin \beta & \cos \beta \end{pmatrix}, \quad R_w = \begin{pmatrix} \cos \theta_w & -\sin \theta_w \\ \sin \theta_w & \cos \theta_w \end{pmatrix}, \quad (S5)$$

with θ_w being the weak mixing angle. Here R_β diagonalizes the hidden sector mass squared matrix while R_w diagonalizes the standard model mass squared matrix, and the diagonalization gives

$$R^T M^2 R = M_D^2 \equiv \text{diag}(m_{\gamma'}^2, m_{Z'}^2, 0, m_Z^2). \quad (S6)$$

Since the mass square matrix is now diagonal, it is a good starting point to diagonalize and normalize the kinetic energy matrix. This is a bit non-trivial and requires several steps which we outline below. In the basis (D, C, B, A_3) , the kinetic Lagrangian is given by

$$\mathcal{L}_{\text{KE}} = -\frac{1}{4}(D^2 + C^2 + B^2 + A_3^2) - \frac{1}{4}(2\delta_1 BC + 2\delta_2 CD), \quad (\text{S7})$$

where we use an abbreviated notation so that $B^2 = B_{\mu\nu}B^{\mu\nu}$, $BC = B_{\mu\nu}C^{\mu\nu}$, etc. Next we write \mathcal{L}_{KE} in the basis $(D^{(1)}, C^{(1)}, B^{(0)}, A_3^{(0)})$ in which the mass square matrix of the gauge bosons is diagonal. Thus, using

$$\begin{pmatrix} D \\ C \end{pmatrix} = R_\beta \begin{pmatrix} D^{(1)} \\ C^{(1)} \end{pmatrix}, \quad \begin{pmatrix} B \\ A_3 \end{pmatrix} = R_w \begin{pmatrix} B^{(0)} \\ A_3^{(0)} \end{pmatrix}. \quad (\text{S8})$$

allows us to write \mathcal{L}_{KE} as

$$\begin{aligned} \mathcal{L}_{\text{KE}} = & -\frac{1}{4}(D^{(1)2} + C^{(1)2} + B^{(0)2} + A_3^{(0)2}) - \frac{1}{2}\delta_1(B^{(0)} \cos \theta_w - A_3^{(0)} \sin \theta_w)(D^{(1)} \sin \beta + C^{(1)} \cos \beta) \\ & - \frac{1}{2}\delta_2(D^{(1)} \sin \beta + C^{(1)} \cos \beta)(D^{(1)} \cos \beta - C^{(1)} \sin \beta). \end{aligned} \quad (\text{S9})$$

The diagonal kinetic terms for $D^{(1)}$ and $C^{(1)}$ have the form

$$-\frac{1}{4}D^{(1)2}(1 + \delta_2 \sin 2\beta) - \frac{1}{4}C^{(1)2}(1 - \delta_2 \sin 2\beta). \quad (\text{S10})$$

To normalize them to unity we make a transformation from the basis $V^{(1)T} = (D^{(1)}, C^{(1)}, B^{(0)}, A_3^{(0)})$ to $V^{(2)T} = (D^{(2)}, C^{(2)}, B^{(0)}, A_3^{(0)})$ so that

$$V^{(1)} = K_1 V^{(2)}, \quad K_1 = \begin{pmatrix} \frac{1}{\sqrt{1+\delta_2 \sin 2\beta}} & 0 & 0 & 0 \\ 0 & \frac{1}{\sqrt{1-\delta_2 \sin 2\beta}} & 0 & 0 \\ 0 & 0 & 1 & 0 \\ 0 & 0 & 0 & 1 \end{pmatrix}, \quad (\text{S11})$$

where

$$\bar{\delta}_2 = \frac{\delta_2 \cos 2\beta}{\sqrt{1 - \delta_2^2 \sin^2 2\beta}}. \quad (\text{S12})$$

After the transformation, \mathcal{L}_{KE} in the $V^{(2)}$ basis has the form

$$\mathcal{L}_{\text{KE}} = -\frac{1}{4}(D^{(2)2} + C^{(2)2} + B^{(0)2} + A_3^{(0)2}) - \frac{1}{2}(\delta_1^+ D^{(2)} + \delta_1^- C^{(2)})(B^{(0)} \cos \theta_w - A_3^{(0)} \sin \theta_w) - \frac{1}{2}\bar{\delta}_2 C^{(2)} D^{(2)}, \quad (\text{S13})$$

where

$$\delta_1^+ = \frac{\delta_1 \sin \beta}{\sqrt{1 + \delta_2 \sin 2\beta}}, \quad \delta_1^- = \frac{\delta_1 \cos \beta}{\sqrt{1 - \delta_2 \sin 2\beta}}. \quad (\text{S14})$$

We now note that there is a $C^{(2)}D^{(2)}$ mixing term in Eq. (S13) which can be removed by an $GL(2, \mathbb{R})$ transformation. We do this by going from the basis $V^{(2)}$ to $V^{(3)T} = (D^{(3)}, C^{(3)}, B^{(0)}, A_3^{(0)})$ so that

$$V^{(2)} = K_2 V^{(3)}, \quad K_2 = \begin{pmatrix} 1 & -s_{\bar{\delta}_2} & 0 & 0 \\ 0 & c_{\bar{\delta}_2} & 0 & 0 \\ 0 & 0 & 1 & 0 \\ 0 & 0 & 0 & 1 \end{pmatrix}, \quad (\text{S15})$$

where

$$s_{\bar{\delta}_2} = \frac{\bar{\delta}_2}{\sqrt{1 - \bar{\delta}_2^2}}, \quad c_{\bar{\delta}_2} = \frac{1}{\sqrt{1 - \bar{\delta}_2^2}}. \quad (\text{S16})$$

In the $V^{(3)}$ basis \mathcal{L}_{KE} becomes

$$\begin{aligned} \mathcal{L}_{\text{KE}} = & -\frac{1}{4}(D^{(3)^2} + C^{(3)^2} + B^{(0)^2} + A_3^{(0)^2}) - \frac{1}{2}\delta_1^- C^{(3)}(B^{(0)} \cos \theta_w - A_3^{(0)} \sin \theta_w) \\ & - \frac{1}{2}\delta' D^{(3)}(B^{(0)} \cos \theta_w - A_3^{(0)} \sin \theta_w), \end{aligned} \quad (\text{S17})$$

where

$$\delta' \equiv \delta_1^+ c_{\delta_2} - \delta_1^- s_{\delta_2}. \quad (\text{S18})$$

We note that while there are no kinetic mixing terms between $C^{(3)}$ and $D^{(3)}$, there are kinetic mixing terms between them and the fields $B^{(0)}$ and $A_3^{(0)}$. The mixing term between $D^{(3)}$ and $B^{(0)}$ can be removed by the transformation

$$V^{(3)} = K_3 V^{(4)}, \quad K_3 = \begin{pmatrix} 1 & 0 & -s_{\delta_3} & 0 \\ 0 & 1 & 0 & 0 \\ 0 & 0 & c_{\delta_3} & 0 \\ 0 & 0 & 0 & 1 \end{pmatrix}, \quad (\text{S19})$$

where $V^{(4)^T} = (D^{(4)}, C^{(3)}, B^{(1)}, A_3^{(0)})$, s_{δ_3} and c_{δ_3} are defined similar to Eq. (S16) and δ_3 is defined by

$$\delta_3 \equiv \delta' \cos \theta_w. \quad (\text{S20})$$

In the $V^{(4)}$ basis the Lagrangian takes the form

$$\begin{aligned} \mathcal{L}_{\text{KE}} = & -\frac{1}{4}(D^{(4)^2} + C^{(3)^2} + B^{(1)^2} + A_3^{(0)^2}) - \frac{1}{2}\delta_1^- C^{(3)}(B^{(1)} c_{\delta_3} \cos \theta_w - A_3^{(0)} \sin \theta_w) \\ & - \frac{1}{2}\delta' D^{(4)}(B^{(1)} c_{\delta_2} \cos \theta_w - A_3^{(0)} \sin \theta_w) + \frac{1}{2}\delta' s_{\delta_3} B^{(1)}(-B^{(1)} s_{\delta_3} \cos \theta_w - A_3^{(0)} \sin \theta_w). \end{aligned} \quad (\text{S21})$$

A mixing term between $D^{(4)}$ and $A_3^{(0)}$ exists which can be removed by the transformation

$$V^{(4)} = K_4 V^{(5)}, \quad K_4 = \begin{pmatrix} 1 & 0 & 0 & -s_{\delta_4} \\ 0 & 1 & 0 & 0 \\ 0 & 0 & 1 & 0 \\ 0 & 0 & 0 & c_{\delta_4} \end{pmatrix}, \quad (\text{S22})$$

where $V^{(5)}$ is given by $V^{(5)^T} = (D^{(5)}, C^{(3)}, B^{(1)}, A_3^{(1)})$ and where s_{δ_4} and c_{δ_4} are defined as in Eq. (S16) and

$$\delta_4 \equiv -\delta' \sin \theta_w. \quad (\text{S23})$$

In the $V^{(5)}$ basis, \mathcal{L}_{KE} takes the form

$$\begin{aligned} \mathcal{L}_{\text{KE}} = & -\frac{1}{4}(D^{(5)^2} + C^{(3)^2} + B^{(1)^2} + A_3^{(1)^2}) - \frac{1}{2}(B^{(1)} c_{\delta_3} \cos \theta_w - A_3^{(1)} c_{\delta_4} \sin \theta_w) \delta_1^- C^{(3)} \\ & - \frac{1}{2} \sin \theta_w \delta' \delta_3 c_{\delta_4} A_3^{(1)} B^{(1)}. \end{aligned} \quad (\text{S24})$$

Next we look at the kinetic mixing of $(C^{(3)}, B^{(1)})$. This mixing can be removed by the transformation

$$V^{(5)} = K_5 V^{(6)}, \quad K_5 = \begin{pmatrix} 1 & 0 & 0 & 0 \\ 0 & 1 & -s_{\delta_5} & 0 \\ 0 & 0 & c_{\delta_5} & 0 \\ 0 & 0 & 0 & 1 \end{pmatrix}. \quad (\text{S25})$$

Here $V^{(6)^T} = (D^{(5)}, C^{(4)}, B^{(2)}, A_3^{(1)})$ and

$$\delta_5 = \delta_1^- c_{\delta_3} \cos \theta_w, \quad (\text{S26})$$

where s_{δ_5} and c_{δ_5} are defined as in Eq. (S16). After the transformation the kinetic energy Lagrangian in the $V^{(5)}$ basis has the form

$$\mathcal{L}_{\text{KE}} = -\frac{1}{4}(D^{(5)^2} + C^{(4)^2} + B^{(2)^2} + A_3^{(1)^2}) + \frac{1}{2}\sin\theta_w\delta_1^-c_{\delta_4}A_3^{(1)}(C^{(4)} - s_{\delta_5}B^{(2)}) - \frac{1}{2}\sin\theta_w\delta'_3\delta_3c_{\delta_4}c_{\delta_5}A_3^{(1)}B^{(2)}. \quad (\text{S27})$$

Next we examine the kinetic mixing of the fields $(C^{(4)}, A_3^{(1)})$. This mixing term can be eliminated by the transformation

$$V^{(6)} = K_6 V^{(7)}, \quad K_6 = \begin{pmatrix} 1 & 0 & 0 & 0 \\ 0 & 1 & 0 & -s_{\delta_6} \\ 0 & 0 & 1 & 0 \\ 0 & 0 & 0 & c_{\delta_6} \end{pmatrix}, \quad (\text{S28})$$

where $V^{(7)^T} = (D^{(5)}, C^{(5)}, B^{(2)}, A_3^{(2)})$ and where δ_6 is defined by

$$\delta_6 = -\delta_1^- c_{\delta_4} \sin\theta_w, \quad (\text{S29})$$

and s_{δ_6} and c_{δ_6} are defined as usual.

After the transformation the kinetic energy Lagrangian in the $V^{(7)}$ basis has the form

$$\mathcal{L}_{\text{KE}} = -\frac{1}{4}(D^{(5)^2} + C^{(5)^2} + B^{(2)^2} + A_3^{(2)^2}) + \frac{1}{2}\delta_7 B^{(2)} A_3^{(2)}, \quad (\text{S30})$$

where

$$\delta_7 = \sin\theta_w\delta_1^-c_{\delta_4}c_{\delta_6}s_{\delta_5} + \sin\theta_w\delta'_3c_{\delta_4}c_{\delta_6}c_{\delta_5}s_{\delta_3}. \quad (\text{S31})$$

We are now left with the last kinetic mixing term involving the fields $B^{(2)}$ and $A_3^{(2)}$. To eliminate this mixing we make the final transformation

$$V^{(7)} = K_7 V^{(8)}, \quad K_7 = \begin{pmatrix} 1 & 0 & 0 & 0 \\ 0 & 1 & 0 & 0 \\ 0 & 0 & 1 & -s_{\delta_7} \\ 0 & 0 & 0 & c_{\delta_7} \end{pmatrix}, \quad (\text{S32})$$

where $V^{(8)^T} = (D^{(5)}, C^{(5)}, B^{(3)}, A_3^{(3)})$. In the basis $V^{(8)}$ the kinetic energy for all the gauge fields is in the canonical form so that

$$\mathcal{L}_{\text{KE}} = -\frac{1}{4}(D^{(5)^2} + C^{(5)^2} + B^{(3)^2} + A_3^{(3)^2}). \quad (\text{S33})$$

The free Lagrangian in the $V^{(8)}$ basis is then

$$\mathcal{L} = -\frac{1}{4}V^{(8)^T}V^{(8)} - \frac{1}{2}V^{(8)^T}K^T M_D^2 K V^{(8)}, \quad (\text{S34})$$

with

$$K \equiv K_1 K_2 K_3 K_4 K_5 K_6 K_7. \quad (\text{S35})$$

As discussed in the beginning of this section we now make the expansion of Eq. (S3). Below we exhibit K and ΔM^2 in the limit $\delta_1, \delta_2 \ll 1$. In this case $s_{\delta_1} \sim \delta_1, c_{\delta_1} \sim 1$, etc. and K and ΔM^2 have the following form

$$K \sim \begin{pmatrix} 1 & -\bar{\delta}_2 & -\delta_3 & -\delta_4 \\ 0 & 1 & -\delta_5 & -\delta_6 \\ 0 & 0 & 1 & -\delta_7 \\ 0 & 0 & 0 & 1 \end{pmatrix}, \quad \Delta M^2 = \begin{pmatrix} 0 & -m_{\gamma'}^2 \bar{\delta}_2 & -m_{\gamma'}^2 \delta_3 & -m_{\gamma'}^2 \delta_4 \\ -m_{\gamma'}^2 \bar{\delta}_2 & 0 & -m_{Z'}^2 \delta_5 & -m_{\gamma'}^2 \delta_6 \\ -m_{\gamma'}^2 \delta_3 & -m_{Z'}^2 \delta_5 & 0 & 0 \\ -m_{\gamma'}^2 \delta_4 & -m_{\gamma'}^2 \delta_6 & 0 & 0 \end{pmatrix}. \quad (\text{S36})$$

The interactions relevant for our computation arise from ΔM^2 and the relation

$$V^{(1)} = K V^{(8)}. \quad (\text{S37})$$

Eqs. (S36) and (S37) and non-degenerate perturbation theory is utilized in the computation of couplings of the visible sector with the hidden sector. This is discussed in the next section.

DARK PHOTON γ' AND DARK Z' COUPLINGS WITH SM PARTICLES

To compute the couplings proportional to δ_1 and δ_2 that arise due to the kinetic and Stueckelberg mass mixings, we use first order non-degenerate perturbation theory using ΔM^2 given in Eq. (S36) as the perturbation. Thus, to first order perturbation in ΔM^2 , the neutral currents of Eq. (2) which involve the vector and axial-vector couplings of the dark photon, the dark Z' and the SM gauge bosons are given by

$$v_f = T_{3f} - 2Q_f \sin^2 \theta_w, \quad (\text{S38})$$

$$a_f = T_{3f}, \quad (\text{S39})$$

$$v'_f = -Q_f \sin 2\theta_w \cos \theta_w (1 + \epsilon_z^2) \delta_1 \left[1 - \left(1 - \frac{T_{3f}}{2Q} \right) \frac{m_{Z'}^2}{m_W^2} \right], \quad (\text{S40})$$

$$a'_f = -\delta_1 T_{3f} \sin \theta_w \epsilon_z^2 (1 + \epsilon_z^2), \quad (\text{S41})$$

$$v''_f = Q_f \sin 2\theta_w \cos \theta_w (1 + \epsilon_{\gamma'}^2) \left[1 - \left(1 - \frac{T_{3f}}{2Q} \right) \frac{m_{\gamma'}^2}{m_W^2} \right] \delta_1 (\delta_2 - \sin \beta), \quad (\text{S42})$$

$$a''_f = T_{3f} \sin \theta_w \epsilon_{\gamma'}^2 (1 + \epsilon_{\gamma'}^2) \delta_1 (\delta_2 - \sin \beta), \quad (\text{S43})$$

where $\epsilon_z = m_{Z'}/m_Z$ and $\epsilon_{\gamma'} = m_{\gamma'}/m_Z$. The relevant couplings with the visible sector are summarized in Tables S1 and S2. Thus Table S1 gives the couplings of Z and Z' to the visible sector fermions $f\bar{f}$ and Table S2 gives the coupling of γ' to $f\bar{f}$.

TABLE S1: The $Z \rightarrow f\bar{f}$ and $Z' \rightarrow f\bar{f}$ vertices. In the above, $\epsilon_z = m_{Z'}/m_Z$ and m_W is the W boson mass.

f	Q_f	v_f	a_f	v'_f	a'_f
ν_e, ν_μ, ν_τ	0	$\frac{1}{2}$	$\frac{1}{2}$	$-\frac{1}{2} \sin \theta_w \epsilon_z^2 (1 + \epsilon_z^2) \delta_1$	$-\frac{1}{2} \sin \theta_w \epsilon_z^2 (1 + \epsilon_z^2) \delta_1$
e, μ, τ	-1	$-\frac{1}{2} + 2 \sin^2 \theta_w$	$-\frac{1}{2}$	$\sin 2\theta_w \cos \theta_w \left(1 - \frac{3m_{Z'}^2}{4m_W^2} \right) (1 + \epsilon_z^2) \delta_1$	$\frac{1}{2} \sin \theta_w \epsilon_z^2 (1 + \epsilon_z^2) \delta_1$
u, c, t	$\frac{2}{3}$	$\frac{1}{2} - \frac{4}{3} \sin^2 \theta_w$	$\frac{1}{2}$	$-\frac{2}{3} \sin 2\theta_w \cos \theta_w \left(1 - \frac{5m_{Z'}^2}{8m_W^2} \right) (1 + \epsilon_z^2) \delta_1$	$-\frac{1}{2} \sin \theta_w \epsilon_z^2 (1 + \epsilon_z^2) \delta_1$
d, s, b	$-\frac{1}{3}$	$-\frac{1}{2} + \frac{2}{3} \sin^2 \theta_w$	$-\frac{1}{2}$	$\frac{1}{3} \sin 2\theta_w \cos \theta_w \left(1 - \frac{m_{Z'}^2}{4m_W^2} \right) (1 + \epsilon_z^2) \delta_1$	$\frac{1}{2} \sin \theta_w \epsilon_z^2 (1 + \epsilon_z^2) \delta_1$

TABLE S2: The $\gamma' \rightarrow f\bar{f}$ vertices. In the above, $\epsilon_{\gamma'} = m_{\gamma'}/m_Z$.

f	Q_f	v''_f	a''_f
ν_e, ν_μ, ν_τ	0	$\frac{1}{2} \sin \theta_w \epsilon_{\gamma'}^2 (1 + \epsilon_{\gamma'}^2) \delta_1 (\delta_2 - s_\beta)$	$\frac{1}{2} \sin \theta_w \epsilon_{\gamma'}^2 (1 + \epsilon_{\gamma'}^2) \delta_1 (\delta_2 - s_\beta)$
e, μ, τ	-1	$\sin 2\theta_w \cos \theta_w \left(1 - \frac{3m_{\gamma'}^2}{4m_W^2} \right) (1 + \epsilon_{\gamma'}^2) \delta_1 (s_\beta - \delta_2)$	$-\frac{1}{2} \sin \theta_w \epsilon_{\gamma'}^2 (1 + \epsilon_{\gamma'}^2) \delta_1 (\delta_2 - s_\beta)$
u, c, t	$\frac{2}{3}$	$\frac{2}{3} \sin 2\theta_w \cos \theta_w \left(1 - \frac{5m_{\gamma'}^2}{8m_W^2} \right) (1 + \epsilon_{\gamma'}^2) \delta_1 (\delta_2 - s_\beta)$	$\frac{1}{2} \sin \theta_w \epsilon_{\gamma'}^2 (1 + \epsilon_{\gamma'}^2) \delta_1 (\delta_2 - s_\beta)$
d, s, b	$-\frac{1}{3}$	$\frac{1}{3} \sin 2\theta_w \cos \theta_w \left(1 - \frac{m_{\gamma'}^2}{4m_W^2} \right) (1 + \epsilon_{\gamma'}^2) \delta_1 (s_\beta - \delta_2)$	$-\frac{1}{2} \sin \theta_w \epsilon_{\gamma'}^2 (1 + \epsilon_{\gamma'}^2) \delta_1 (\delta_2 - s_\beta)$

The triple gauge boson couplings of γ', Z', Z are given by are

$$WW\gamma' : -ig_2 \cos \theta_w \sin \theta_w (1 + \epsilon_{\gamma'}^2) \delta_1 (\delta_2 - \sin \beta). \quad (\text{S44})$$

$$WWZ' : ig_2 \cos \theta_w \sin \theta_w (1 + \epsilon_z^2) \delta_1, \quad (\text{S45})$$

$$WWZ : -ig_2 \cos \theta_w. \quad (\text{S46})$$

Couplings in the limit of large δ_2 : Some of the processes such as the lifetime of the dark photon require only that the product $\delta_1\delta_2$ be small which could be achieved by δ_1 being small while δ_2 is $\mathcal{O}(1)$ size. Thus we list below the vector and axial-vector couplings in the limit of small δ_1 and β while δ_2 is not necessarily small

$$v_f = T_{3f} - 2Q_f \sin^2 \theta_w + \frac{Q_f \delta_1 \delta_2 \sin \theta_w \sin 2\theta_w (\delta_2 - \sin \beta + \delta_2^2 \sin \beta)}{\sqrt{1 - \delta_2^2}}, \quad (\text{S47})$$

$$a_f = T_{3f}, \quad (\text{S48})$$

$$v'_f = -Q_f \sin 2\theta_w \cos \theta_w (1 + \epsilon_z^2 + \epsilon_{\gamma'}^2 \delta_2^2) \delta_1 \left[\frac{m_{Z'}^2}{m_{Z'}^2 + m_{\gamma'}^2 \delta_2^2} - \left(1 - \frac{T_{3f}}{2Q_f} \right) \frac{m_{Z'}^2}{m_W^2} \right] \\ \times \left[(1 + \delta_2 \sin \beta) + \frac{m_{\gamma'}^2}{m_{Z'}^2} \frac{\delta_2^2 (1 + \delta_2 \sin \beta) - \delta_2 \sin \beta}{\sqrt{1 - \delta_2^2}} \right], \quad (\text{S49})$$

$$a'_f = -\delta_1 T_{3f} \sin \theta_w (1 + \epsilon_z^2 + \delta_2^2 \epsilon_{\gamma'}^2) \left[\epsilon_z^2 (1 + \delta_2 \sin \beta) + \epsilon_{\gamma'}^2 \frac{\delta_2^2 (1 + \delta_2 \sin \beta) - \delta_2 \sin \beta}{\sqrt{1 - \delta_2^2}} \right], \quad (\text{S50})$$

$$v''_f = Q_f \sin 2\theta_w \cos \theta_w (1 + \epsilon_{\gamma'}^2) \left[1 - \left(1 - \frac{T_{3f}}{2Q_f} \right) \frac{m_{\gamma'}^2}{m_W^2} \right] \frac{\delta_1 (\delta_2 - \sin \beta + \delta_2^2 \sin \beta)}{\sqrt{1 - \delta_2^2}}, \quad (\text{S51})$$

$$a''_f = T_{3f} \sin \theta_w \epsilon_{\gamma'}^2 (1 + \epsilon_{\gamma'}^2) \frac{\delta_1 (\delta_2 - \sin \beta + \delta_2^2 \sin \beta)}{\sqrt{1 - \delta_2^2}}. \quad (\text{S52})$$

The couplings with the D fermions become

$$\gamma' D \bar{D} : g_X \frac{m_{\gamma'}^2 \delta_2}{m_{Z'}^2 - m_{\gamma'}^2 (1 - \delta_2^2)}, \quad (\text{S53})$$

$$Z' D \bar{D} : g_X, \quad (\text{S54})$$

$$\gamma D \bar{D} : -g_X \frac{m_{\gamma'}^2 \delta_1 \delta_2 \cos \theta_w}{m_{Z'}^2 + m_{\gamma'}^2 \delta_2^2} \left[\delta_2 (1 + \beta \delta_2) + \frac{\beta - \delta_2 - \beta \delta_2^2}{\sqrt{1 - \delta_2^2}} \right], \quad (\text{S55})$$

$$Z D \bar{D} : g_X \delta_1 \sin \theta_w (1 + \epsilon_z^2 + \delta_2^2 \epsilon_{\gamma'}^2) \left[(1 + \beta \delta_2) (1 + \delta_2^2 \epsilon_{\gamma'}^2) + \frac{\delta_2 \epsilon_{\gamma'}^2}{\sqrt{1 - \delta_2^2}} (\beta - \delta_2 - \beta \delta_2^2) \right], \quad (\text{S56})$$

and the triple gauge boson couplings take the form

$$WWZ : -ig_2 \cos \theta_w \left[1 + \frac{\sin \theta_w \tan \theta_w \delta_1 \delta_2 (\beta \delta_2^2 + \delta_2 - \beta)}{\sqrt{1 - \delta_2^2}} \right], \quad (\text{S57})$$

$$WWZ' : ig_2 \cos \theta_w \sin \theta_w \frac{\delta_1 (1 + \epsilon_z^2 + \epsilon_{\gamma'}^2 \delta_2^2)}{m_{Z'}^2 + m_{\gamma'}^2 \delta_2^2} \left[m_{Z'}^2 (1 + \delta_2 \beta) + \frac{m_{\gamma'}^2 \delta_2 (\beta \delta_2^2 + \delta_2 - \beta)}{\sqrt{1 - \delta_2^2}} \right], \quad (\text{S58})$$

$$WW\gamma' : ig_2 \cos \theta_w \sin \theta_w (1 + \epsilon_{\gamma'}^2) \frac{\delta_1 (\delta_2 - s_\beta + \beta \delta_2^2)}{\sqrt{1 - \delta_2^2}}. \quad (\text{S59})$$

TEMPERATURE EVOLUTION IN DARK SECTORS VS IN THE VISIBLE SECTOR

In this section we derive the evolution equations for temperatures T_1 and T_2 in the dark sectors and T in the visible sector, i.e., T_1/T and T_2/T as a function of T . However, for numerical integration purposes it is found more convenient to use T_1 as the reference temperature. Thus we are interested in deriving the evolution equations for $d\eta/dT_1$ and $d\zeta/dT_1$ where we recall that η and ζ are defined so that

$$T \equiv \eta T_1, \quad T_2 \equiv \zeta T_1. \quad (\text{S60})$$

To this end we look at the equations for the energy densities in the visible and the hidden sectors. In the analysis, we encounter the quantity $d\rho/dT_1$. The main difficulty in computing the quantity $d\rho/dT_1$ is that ρ is constituted of

three parts, $\rho = \rho_v + \rho_1 + \rho_2$ which depends on three temperatures i.e., ρ_v is controlled by T , ρ_1 is controlled by T_1 and ρ_2 is controlled by T_2 . Thus we need to express $d\rho_v/dT_1$ in terms of $d\rho_v/dT$ and $d\rho_2/dT_1$ in terms of $d\rho_2/dT_2$. Using the definitions of η and ζ we can write

$$\frac{d\rho_v}{dT_1} = \left(\eta + T_1 \frac{d\eta}{dT_1} \right) \frac{d\rho_v}{dT}, \quad \text{and} \quad \frac{d\rho_2}{dT_1} = \left(\zeta + T_1 \frac{d\zeta}{dT_1} \right) \frac{d\rho_2}{dT}. \quad (\text{S61})$$

This means that a determination of $d\rho_v/dT_1$ and $d\rho_2/dT_1$ requires $d\eta/dT_1$ and $d\zeta/dT_2$. Next, we derive the evolution equations for these quantities.

We note that ρ_v, ρ_1, ρ_2 satisfy the following evolution equations

$$\begin{aligned} \frac{d\rho_v}{dt} + 4\rho_v H &= j_v, \\ \frac{d\rho_1}{dt} + 4\rho_1 H &= j_1, \\ \frac{d\rho_2}{dt} + 4\rho_2 H &= j_2, \end{aligned} \quad (\text{S62})$$

where j_v, j_1, j_2 are the corresponding sources. Instead of time we will use temperature so we will need to convert derivatives with respect to time to derivatives with respect to temperature. We note now that for any given temperatures T_i the time derivative of temperature is given by

$$\frac{dT_i}{dt} = -\frac{4H\rho}{\frac{d\rho}{dT_i}}. \quad (\text{S63})$$

As discussed above, we choose T_1 to be the reference temperature and the evolution equation for ρ_v in this case can be written as

$$j_v - 4\rho_v H = -\frac{4H\rho}{\frac{d\rho}{dT_1}} \frac{d\rho_v}{dT_1}. \quad (\text{S64})$$

From Eq. (S64) we can deduce that

$$\frac{d\rho_v}{dT_1} = \frac{4\rho_v H - j_v}{4H(\rho_1 + \rho_2) + j_v} \left(\frac{d\rho_1}{dT_1} + \frac{d\rho_2}{dT_1} \right). \quad (\text{S65})$$

In a similar fashion starting with the equation for $d\rho_2/dt$ we can deduce

$$\frac{d\rho_2}{dT_1} = \frac{4\rho_2 H - j_2}{4H(\rho_1 + \rho_v) + j_2} \left(\frac{d\rho_1}{dT_1} + \frac{d\rho_v}{dT_1} \right). \quad (\text{S66})$$

Eqs. (S65) and (S66) are two coupled equations involving $d\rho_v/dT_1$ and $d\rho_2/dT_1$ which give the solution

$$\frac{d\rho_v}{dT_1} = \frac{(AB + A)}{(1 - AB)} \frac{d\rho_1}{dT_1}, \quad \text{and} \quad \frac{d\rho_2}{dT_1} = \frac{(AB + B)}{(1 - AB)} \frac{d\rho_1}{dT_1}, \quad (\text{S67})$$

where

$$A = \frac{4\rho_v H - j_v}{4H(\rho_1 + \rho_2) + j_v}, \quad B = \frac{4\rho_2 H - j_2}{4H(\rho_v + \rho_1) + j_2}. \quad (\text{S68})$$

Using Eqs. (S61) and (S67) one can then obtain the relations

$$\frac{d\eta}{dT_1} = -\frac{\eta}{T_1} + \frac{(AB + A)}{(1 - AB)} \frac{y}{T_1 \frac{d\rho_v}{dT}}, \quad \text{and} \quad \frac{d\zeta}{dT_1} = -\frac{\zeta}{T_1} + \frac{(AB + B)}{(1 - AB)} \frac{y}{T_1 \frac{d\rho_2}{dT_2}}. \quad (\text{S69})$$

Using the fact that $j_v + j_1 + j_2 = 0$, eliminating j_v in favor of j_1 and j_2 and inserting Eq. (S68) in Eq. (S69), one can further simplify Eq. (S69) to obtain $d\eta/dT_1$ and $d\zeta/dT_1$ as shown in Eqs. (11) and (12). The source terms j_1 and j_2 are given by

$$\begin{aligned} j_1 = \sum_i & [2Y_i(T)^2 J(i\bar{i} \rightarrow D\bar{D})(T) + 2Y_i(T)^2 J(i\bar{i} \rightarrow Z'Z')(T) + Y_i(T)^2 J(i\bar{i} \rightarrow Z')(T) \\ & + 2Y_{\gamma'}^2 J(\gamma'\gamma' \rightarrow D\bar{D})(T_2) - \frac{1}{2}Y_D^2 J(D\bar{D} \rightarrow \gamma'\gamma')(T_1) - \frac{1}{2}Y_D^2 J(D\bar{D} \rightarrow Z'\gamma')(T_1) \\ & + Y_{Z'}Y_{\gamma'} J(Z'\gamma' \rightarrow D\bar{D})(T_1, T_2)] s^2 - Y_{Z'} J(Z' \rightarrow i\bar{i})(T_1) s, \end{aligned} \quad (\text{S70})$$

$$\begin{aligned}
j_2 = \sum_i & [Y_i(T)^2 J(i\bar{i} \rightarrow \gamma')(T) + Y_D^2 J(D\bar{D} \rightarrow \gamma'\gamma')(T_1) - Y_{\gamma'}^2 J(\gamma'\gamma' \rightarrow D\bar{D})(T_2) \\
& + 2Y_i(T)^2 J(i\bar{i} \rightarrow \gamma'\gamma')(T) - Y_{\gamma'}^2 J(\gamma'\gamma' \rightarrow i\bar{i})(T_2) + \frac{1}{2}Y_D^2 J(D\bar{D} \rightarrow Z'\gamma')(T_1) \\
& - Y_{Z'}Y_{\gamma'} J(Z'\gamma' \rightarrow D\bar{D})(T_1, T_2)] s^2 - Y_{\gamma'} J(\gamma' \rightarrow \nu\bar{\nu})(T_2)s,
\end{aligned} \tag{S71}$$

with

$$n_i(T)^2 J(i\bar{i} \rightarrow D\bar{D})(T) = \frac{T}{32\pi^4} \int_{4m_D^2}^{\infty} ds \sigma_{D\bar{D} \rightarrow i\bar{i}} s(s - s_i) K_2(\sqrt{s}/T), \tag{S72}$$

$$n_i(T)^2 J(i\bar{i} \rightarrow Z')(T) = \frac{T}{32\pi^4} \int_{4m_i^2}^{\infty} ds \sigma_{i\bar{i} \rightarrow \gamma'} s(s - s_i) K_2(\sqrt{s}/T), \tag{S73}$$

$$n_D(T_1)^2 J(D\bar{D} \rightarrow \gamma'\gamma')(T_1) = \frac{n_D(T_1)^2}{8m_D^4 T_1 K_2^2(m_D/T_1)} \int_{4m_D^2}^{\infty} ds \sigma_{D\bar{D} \rightarrow \gamma'\gamma'} s(s - 4m_D^2) K_2(\sqrt{s}/T), \tag{S74}$$

$$n_{Z'} J(Z' \rightarrow i\bar{i})(T_1) = n_{Z'} m_{Z'} \Gamma_{Z' \rightarrow i\bar{i}}. \tag{S75}$$

DEDUCTION OF THREE TEMPERATURE BOLTZMANN EQUATIONS

Next we give a deduction of the Boltzmann equations for the case of three heat baths. We will use T_1 as the reference temperature. Let us consider a generic number density n_i . In this case $n_i R^3$ is conserved during the expansion if there is no injection and we have $\frac{d(n_i R^3)}{dt} = 0$ where R is the scale factor, while in the presence of injection one has

$$\frac{dn_i}{dt} + 3Hn_i = C_i, \tag{S76}$$

where C_i represent the integrated collision terms. Next, if $S = sR^3$ is the total entropy, it is conserved which implies that

$$\frac{ds}{dt} + 3Hs = 0. \tag{S77}$$

Using Eqs. (S76) and (S77), and the fact that $n_i = sY_i$, one finds

$$\frac{dY_i}{dt} = \frac{1}{s} C_i. \tag{S78}$$

We can convert this equation to one that uses temperature T_1 rather than time which gives

$$\frac{dY_i}{dT_1} = -\frac{d\rho/dT_1}{4H\rho} \frac{1}{s} C_i, \tag{S79}$$

where $d\rho/dT_1$ is given by

$$\frac{d\rho}{dT_1} = (\eta + T_1\eta') \frac{d\rho_v}{dT} + \frac{d\rho_1}{dT_1} + (\zeta + T_1\zeta') \frac{d\rho_2}{dT_2}. \tag{S80}$$

The Boltzmann equations for $Y_D, Y_{Z'}, Y_{\gamma'}$ may now be written as

$$\begin{aligned}
\frac{dY_D}{dT_1} &= -\frac{d\rho/dT_1}{4H\rho} \frac{1}{s} C_D, \\
\frac{dY_{Z'}}{dT_1} &= -\frac{d\rho/dT_1}{4H\rho} \frac{1}{s} C_{Z'}, \\
\frac{dY_{\gamma'}}{dT_1} &= -\frac{d\rho/dT_1}{4H\rho} \frac{1}{s} C_{\gamma'},
\end{aligned} \tag{S81}$$

where C_D , $C_{Z'}$ and $C_{\gamma'}$ are given by

$$C_D = n_i^2(T) \langle \sigma v \rangle_{i\bar{i} \rightarrow D\bar{D}}(T) + n_{Z'}^2(T_1) \langle \sigma v \rangle_{Z'Z' \rightarrow D\bar{D}}(T_1) - n_D^2(T_1) \langle \sigma v \rangle_{D\bar{D} \rightarrow i\bar{i}}(T_1) \\ - n_D^2(T_1) \langle \sigma v \rangle_{D\bar{D} \rightarrow Z'Z'}(T_1) - n_D^2(T_1) \langle \sigma v \rangle_{D\bar{D} \rightarrow \gamma'\gamma'}(T_1) + n_{\gamma'}^2(T_2) \langle \sigma v \rangle_{\gamma'\gamma' \rightarrow D\bar{D}}(T_2), \quad (\text{S82})$$

$$C_{Z'} = n_i^2(T) \langle \sigma v \rangle_{i\bar{i} \rightarrow Z'}(T) + n_i^2(T) \langle \sigma v \rangle_{i\bar{i} \rightarrow Z'Z'}(T) + n_D^2(T_1) \langle \sigma v \rangle_{D\bar{D} \rightarrow Z'Z'}(T_1) \\ - n_{Z'}^2(T_1) \langle \sigma v \rangle_{Z'Z' \rightarrow i\bar{i}}(T_1) - n_{Z'}^2(T_1) \langle \sigma v \rangle_{Z'Z' \rightarrow D\bar{D}}(T_1) - n_{Z'}(T_1) \langle \Gamma_{Z' \rightarrow i\bar{i}} \rangle(T_1), \quad (\text{S83})$$

$$C_{\gamma'} = n_i^2(T) \langle \sigma v \rangle_{i\bar{i} \rightarrow \gamma'}(T) + n_D^2(T_1) \langle \sigma v \rangle_{D\bar{D} \rightarrow \gamma'\gamma'}(T_1) - n_{\gamma'}(T_2) \langle \sigma v \rangle_{\gamma' \rightarrow i\bar{i}}(T_2) \\ - n_{\gamma'}^2(T_2) \langle \sigma v \rangle_{\gamma'\gamma' \rightarrow D\bar{D}}(T_2). \quad (\text{S84})$$

It is convenient to define

$$\mathcal{J}_D = \frac{C_D}{s^2}, \quad \mathcal{J}_{Z'} = \frac{C_{Z'}}{s^2}, \quad \mathcal{J}_{\gamma'} = \frac{C_{\gamma'}}{s^2}. \quad (\text{S85})$$

$\mathcal{J}_D, \mathcal{J}_{Z'}, \mathcal{J}_{\gamma'}$ appear as source terms in the Boltzmann Eqs. (8), (9), and (10).

In Eqs. (S82), (S83) and (S84) one encounters thermally averaged decay width and thermally averaged cross sections. The thermally averaged decay width is given by

$$\langle \Gamma_{a \rightarrow bc} \rangle = \Gamma_{a \rightarrow bc} \frac{K_1(m_a/T)}{K_2(m_a/T)}, \quad (\text{S86})$$

and the thermally averaged cross-section is given by

$$\langle \sigma v \rangle^{a\bar{a} \rightarrow bc}(T) = \frac{1}{8m_a^4 T K_2^2(m_a/T)} \int_{4m_a^2}^{\infty} ds \, \sigma(s) \sqrt{s} (s - 4m_a^2) K_1(\sqrt{s}/T). \quad (\text{S87})$$

K_1 and K_2 are the modified Bessel functions of the second kind and degrees one and two, respectively. For the case when the annihilating particles have different masses m_1 and m_2 and are at different temperatures T_1 and T_2 , the thermally averaged cross-section becomes

$$\langle \sigma v \rangle_{12 \rightarrow 34}(T_1, T_2) = \frac{1}{4m_1^2 m_2^2 K_2(m_1/T_1) K_2(m_2/T_2)} \int_{(m_1+m_2)^2}^{\infty} ds \, \sigma(s) \sqrt{s(s - (m_1 + m_2)^2)} I(s), \quad (\text{S88})$$

where

$$I(s) = \frac{1}{T_1 - T_2} \int_{\sqrt{s}}^{\infty} dx \, e^{-a_+ x/2} \sinh \left(\frac{a_-}{2} \sqrt{1 - \frac{(m_1 + m_2)^2}{s}} \sqrt{x^2 - s} \right), \quad (\text{S89})$$

and where

$$a_+ = \frac{T_1 + T_2}{T_1 T_2}, \quad a_- = \frac{T_1 - T_2}{T_1 T_2}. \quad (\text{S90})$$

Note that in the limit $T_1 \rightarrow T_2$, $I(s) \rightarrow \frac{\sqrt{s - (m_1 + m_2)^2}}{2T} K_1(\sqrt{s}/T)$ which for $m_1 = m_2$ allows us to recover Eq. (S87) using Eq. (S88). The equilibrium yield of species i is given by

$$Y_i = \frac{n_i^{\text{eq}}}{s} = \frac{g_i}{2\pi^2 s} m_i^2 T K_2(m_i/T). \quad (\text{S91})$$

The hidden sectors degrees of freedom is given by

$$g_1^{\text{eff}} = g_{\text{eff}}^{Z'} + \frac{7}{8} g_{\text{eff}}^D, \quad \text{and} \quad h_1^{\text{eff}} = h_{\text{eff}}^{Z'} + \frac{7}{8} h_{\text{eff}}^D, \quad (\text{S92})$$

$$g_2^{\text{eff}} = g_{\text{eff}}^{\gamma'}, \quad \text{and} \quad h_2^{\text{eff}} = h_{\text{eff}}^{\gamma'}, \quad (\text{S93})$$

where

$$\begin{aligned} g_{\text{eff}}^V &= \frac{45}{\pi^4} \int_{x_V}^{\infty} \frac{\sqrt{x^2 - x_V^2}}{e^x - 1} x^2 dx, \quad \text{and} \quad h_{\text{eff}}^V = \frac{45}{4\pi^4} \int_{x_V}^{\infty} \frac{\sqrt{x^2 - x_V^2}}{e^x - 1} (4x^2 - x_V^2) dx, \\ g_{\text{eff}}^D &= \frac{60}{\pi^4} \int_{x_D}^{\infty} \frac{\sqrt{x^2 - x_D^2}}{e^x + 1} x^2 dx, \quad \text{and} \quad h_{\text{eff}}^D = \frac{15}{\pi^4} \int_{x_D}^{\infty} \frac{\sqrt{x^2 - x_D^2}}{e^x + 1} (4x^2 - x_D^2) dx. \end{aligned} \quad (\text{S94})$$

In Eq. (S94), $V = Z', \gamma'$ and we take $g_{\gamma'} = g_{Z'} = 3$ and $g_D = 4$.

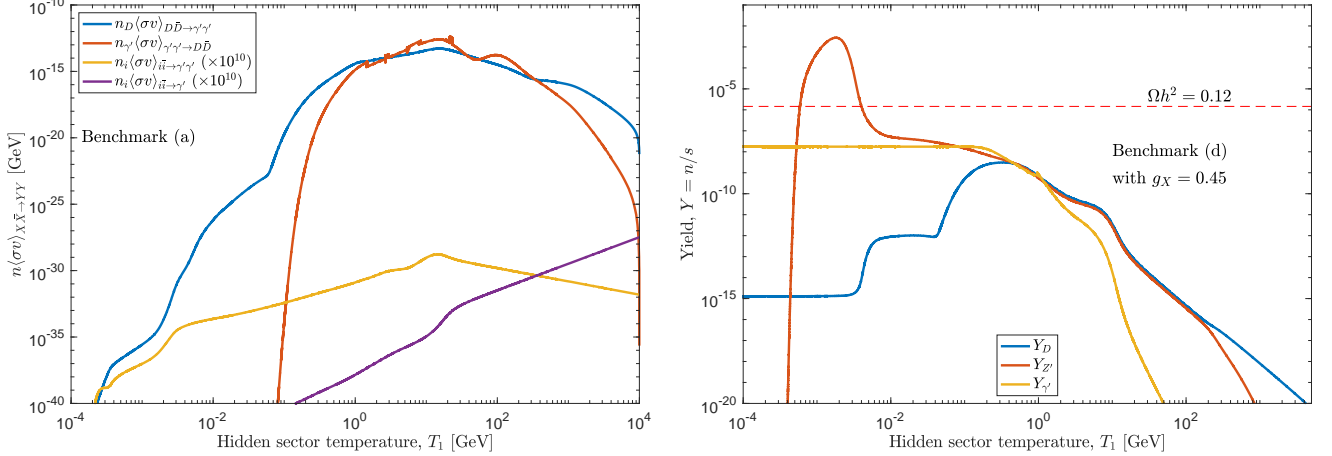


FIG. S2: Left panel: A plot of $n(\sigma v)$ for the processes contributing to the dark photon number density as a function of T_1 . Right panel: The yields of the hidden sector particles showing a diminishing $Y_{\gamma'}$ due to a smaller g_X for benchmark (d).

SATISFACTION OF THE ASTROPHYSICAL CONSTRAINTS

For a dark photon that has direct kinetic mixing with the visible sector, the most stringent limits available come from astrophysical and cosmological sources. Those limits become even stronger when the dark photon is assumed to be the dark matter particle. Thus, measurements of heating rates of the Galactic center cold gas clouds [42], the temperature of the diffuse X-ray background [43] as well as that of the intergalactic medium at the time of He^{++} reionization [44–46] are affected by early $\gamma' \rightarrow 3\gamma$ decays. Further constraints can be derived from energy injection during the dark ages [47] and spectral distortion of the CMB [46]. The presence of a long-lived sub-MeV particle species can contribute to the relativistic number of degrees of freedom ΔN_{eff} during BBN and recombination [48]. All those constraints can exclude a sub-MeV dark photon down to a kinetic mixing coefficient $\mathcal{O}(10^{-13})$.

In the model discussed here, the dark photon resides in a hidden sector X_2 that does not interact directly with the visible sector. Instead, the direct interaction is between the two hidden sectors X_1 and X_2 via kinetic and mass mixings. Since X_1 mixes kinetically with the visible sector, the interaction between X_2 and the visible sector becomes doubly suppressed and all coupling will be proportional to $\delta_1(\delta_2 - \sin\beta)$. The quantity $\sin\beta$ is due to the mass mixing between the hidden sector and such a term can impart millicharges to the D fermions. However, the coupling between the photon and the D fermions is not only suppressed by $\delta_1\delta_2\sin\beta$ but also by the mass ratio as evident from the expression of c_γ in Eq. (6). Therefore even for a modest value of $\sin\beta \sim 10^{-2}$, the millicharges are very small and do not constitute a significant constraint on the model. This doubly suppressed coupling between the dark photon and the SM can alleviate the present constraints mainly from $\gamma' \rightarrow 3\gamma$ as seen in Fig. 5 of the Letter.

It is argued in Ref. [43] that a dark photon with direct kinetic mixing with the SM can only give a subdominant contribution to the relic density and that such an observation can be dismissed if another production mechanism is in effect. The model discussed here presents exactly this counter argument required to produce a dominant dark photon dark matter. The main production mechanism for the dark photon in the current analysis is not via the freeze-in mechanism from the visible sector, $i\bar{i} \rightarrow \gamma'$ and $i\bar{i} \rightarrow \gamma'\gamma'$, because of the doubly suppressed coupling (see left panel of Fig. S2) but rather from interactions between the hidden sector particles. Thus, processes such as $D\bar{D} \rightarrow \gamma'\gamma'$ have cross-sections proportional to $g_X\delta_2$. As shown in Fig. 5, the sizes of g_X and δ_2 are in the required ranges to

produce a dark photon relic density which dominates that of D . A smaller value of g_X will reduce the dark photon yield as expected (see right panel of Fig. S2). We note in passing that the gauge coupling g_X is constrained by the main annihilation channel $D\bar{D} \rightarrow Z'Z' \rightarrow 4e$ from the Planck experiment [49, 50] and for $m_D < 1$ GeV, $g_X > 0.1$ is excluded. However, this constraint does not exist for our model since the relic abundance of our D fermions is negligible. The effect of the forward process $D\bar{D} \rightarrow \gamma'\gamma'$ can be clearly seen in Fig. 2 where the drop in the D fermions yield at a certain temperature is followed by a rise in the yield of γ' . It is worth mentioning that the reverse process $\gamma'\gamma' \rightarrow D\bar{D}$ works on reducing the number density of γ' on the expense of D , but this process shuts off early on as shown in Fig. S2 allowing $D\bar{D} \rightarrow \gamma'\gamma'$ to completely take over for lower temperatures.

DARK PHOTON AND DARK FERMION SCATTERING CROSS SECTIONS AND Z' DECAY WIDTH

As noted in the introduction a strong constraint on dark photon, which is the dominant component of dark matter with the dark fermion being a tiny sub-component, is that of relic density. An analysis of their relic densities involves a variety of cross sections involving the standard model and dark sector particles. We list these below.

1. Processes: $D\bar{D} \rightarrow Z, Z', \gamma' \rightarrow f\bar{f}$

$$\begin{aligned} \sigma^{D\bar{D} \rightarrow f\bar{f}}(s) = & \frac{g_X^2 g_2^2 N_c}{12\pi \cos^2 \theta_w} \left(1 + \frac{2m_D^2}{s} \right) \sqrt{\frac{s - 4m_f^2}{s - 4m_D^2}} \left\{ \frac{[a_f'^2(s - 4m_f^2) + v_f'^2(s + 2m_f^2)]\delta_2^2}{\kappa^2[(s - m_{\gamma'}^2)^2 + m_{\gamma'}^2 \Gamma_{\gamma'}^2]} \right. \\ & + \frac{a_f'^2(s - 4m_f^2) + v_f'^2(s + 2m_f^2)}{(s - m_{Z'}^2)^2 + m_{Z'}^2 \Gamma_{Z'}^2} + \frac{[a_f^2(s - 4m_f^2) + v_f^2(s + 2m_f^2)]\delta_1^2 \sin^2 \theta_w}{(s - m_Z^2)^2 + m_Z^2 \Gamma_Z^2} \\ & + \frac{2\delta_2[a_f' a_f''(s - 4m_f^2) + v_f' v_f''(s + 2m_f^2)]}{\kappa[(s - m_{Z'}^2)^2 + m_{Z'}^2 \Gamma_{Z'}^2][(s - m_{\gamma'}^2)^2 + m_{\gamma'}^2 \Gamma_{\gamma'}^2]} G(s, m_{Z'}, m_{\gamma'}) \\ & + \frac{2\delta_1 \delta_2 [a_f a_f''(s - 4m_f^2) + v_f v_f''(s + 2m_f^2)] \sin \theta_w}{\kappa[(s - m_Z^2)^2 + m_Z^2 \Gamma_Z^2][(s - m_{\gamma'}^2)^2 + m_{\gamma'}^2 \Gamma_{\gamma'}^2]} G(s, m_Z, m_{\gamma'}) \\ & \left. + \frac{2\delta_1 [a_f a_f'(s - 4m_f^2) + v_f v_f'(s + 2m_f^2)] \sin \theta_w}{[(s - m_{Z'}^2)^2 + m_{Z'}^2 \Gamma_{Z'}^2][(s - m_Z^2)^2 + m_Z^2 \Gamma_Z^2]} G(s, m_Z, m_{Z'}) \right\}, \end{aligned} \quad (\text{S95})$$

Here s is the Mandelstam variable which gives the square of the total energy in the CM system. Further, the notation used above is as follows: $f = e, \mu, \tau$: $T_{3f} = -1/2$ and $Q_f = -1$ and for $f = u, c, t$: $T_f^3 = 1/2$ and $Q_f = 2/3$ and for $f = d, s, b$: $T_f^3 = -1/2$ and $Q_f = -1/3$, N_c is the color number and

$$\kappa = -(1 - m_{Z'}^2/m_{\gamma'}^2), \quad (\text{S96})$$

$$G(s, m_1, m_2) = (s - m_1^2)(s - m_2^2) + \Gamma_1 \Gamma_2 m_1 m_2. \quad (\text{S97})$$

2. Processes: $D\bar{D} \rightarrow Z, Z', \gamma' \rightarrow \nu\bar{\nu}$

$$\sigma^{D\bar{D} \rightarrow \nu\bar{\nu}}(s) = \frac{g_X^2 g_2^2 \delta_1^2}{8\pi} \frac{(s + 4m_D^2) \tan^2 \theta_w}{(1 - 4m_D^2/s)^{1/2}} \left[\frac{A}{(s - m_{Z'}^2)(s - m_{\gamma'}^2)} - \frac{1}{(s - m_Z^2)} \right]^2, \quad (\text{S98})$$

where

$$A = \epsilon_z^2 (s - m_{\gamma'}^2) + \frac{\delta_2 \epsilon_{\gamma'}^2 (s - m_{Z'}^2) (\delta_2 - \sin \beta)}{1 - m_{Z'}^2/m_{\gamma'}^2}. \quad (\text{S99})$$

3. Processes: $f\bar{f} \rightarrow Z, Z', \gamma' \rightarrow D\bar{D}$

$$(s - 4m_D^2) \sigma^{D\bar{D} \rightarrow f\bar{f}}(s) = N_c^2 (s - 4m_f^2) \sigma^{f\bar{f} \rightarrow D\bar{D}}(s). \quad (\text{S100})$$

4. Processes: $\nu\bar{\nu} \rightarrow Z, Z', \gamma' \rightarrow D\bar{D}$

$$\sigma^{\nu\bar{\nu} \rightarrow D\bar{D}}(s) = 4 \left(1 - \frac{4m_D^2}{s} \right) \sigma^{D\bar{D} \rightarrow \nu\bar{\nu}}(s). \quad (\text{S101})$$

5. Process: $D\bar{D} \rightarrow Z'Z'$

$$\sigma^{D\bar{D} \rightarrow Z'Z'}(s) = \frac{g_X^4}{8\pi s} \left\{ -\sqrt{\frac{s-4m_{Z'}^2}{s-4m_D^2}} \left[\frac{m_D^2 s + 2m_{Z'}^4 + 4m_D^4}{(s-4m_{Z'}^2)m_D^2 + m_{Z'}^4} \right] \right. \\ \left. + \frac{s^2 + 4m_D^2(s-2m_{Z'}^2) + 4m_{Z'}^4 - 8m_D^4}{(s-2m_{Z'}^2)(s-4m_D^2)} \log B \right\}, \quad (\text{S102})$$

where

$$B = \frac{s-2m_{Z'}^2 + \sqrt{(s-4m_{Z'}^2)(s-4m_D^2)}}{s-2m_{Z'}^2 - \sqrt{(s-4m_{Z'}^2)(s-4m_D^2)}}. \quad (\text{S103})$$

6. Process: $D\bar{D} \rightarrow \gamma'\gamma'$

$$\sigma^{D\bar{D} \rightarrow \gamma'\gamma'}(s) = \left(\frac{\delta_2 M_{\gamma'}^2}{M_{Z'}^2 - M_{\gamma'}^2} \right)^4 \sigma^{D\bar{D} \rightarrow Z'Z'}(s) \Big|_{m_{Z'} \leftrightarrow m_{\gamma'}}. \quad (\text{S104})$$

7. Processes: $D\bar{D} \rightarrow VV$ with $V = Z', \gamma'$

$$8(s-4m_D^2)\sigma^{D\bar{D} \rightarrow VV}(s) = 9(s-4m_V^2)\sigma^{VV \rightarrow D\bar{D}}(s).$$

8. Processes $D\bar{D} \rightarrow Z'\gamma'$

$$\sigma^{D\bar{D} \rightarrow Z'\gamma'}(s) = \frac{\delta_2^2 g_X^4 m_{\gamma'}^4}{4\pi(m_{Z'}^2 - m_{\gamma'}^2)s(s-4m_D^2)} \\ \times \left\{ \frac{4m_D^4 s - 2m_{Z'}m_{\gamma'}s + m_D^2[(m_{Z'}^2 - m_{\gamma'}^2)^2 + s^2]}{m_{Z'}^2 m_{\gamma'}^2 s + m_D^2[m_{\gamma'}^4 + (s-m_{Z'}^2)^2 - 2m_{\gamma'}^2(s+m_{Z'}^2)]} E \right. \\ \left. + [-8m_D^4 + (m_{Z'}^2 + m_{\gamma'}^2)^2 - 4m_D^2(m_{Z'}^2 - m_{\gamma'}^2 - s) + s^2] \log F \right\}, \quad (\text{S105})$$

where

$$E = \sqrt{\left(1 - \frac{4m_D^2}{s}\right) \left[m_{\gamma'}^4 + (s-m_{Z'}^2)^2 - 2m_{\gamma'}^2(s+m_{Z'}^2)\right]}, \quad (\text{S106})$$

$$F = \frac{m_{\gamma'}^2 + m_{Z'}^2 - s + E}{m_{\gamma'}^2 + m_{Z'}^2 - s - E}. \quad (\text{S107})$$

9. Processes $Z'\gamma' \rightarrow D\bar{D}$

$$\sigma^{Z'\gamma' \rightarrow D\bar{D}}(s) = \frac{4s(s-4m_D^2)}{9[(m_{\gamma'}^2 + m_{Z'}^2 - s)^2 - 4m_{\gamma'}^2 m_{Z'}^2]} \sigma^{D\bar{D} \rightarrow Z'\gamma'}(s) \quad (\text{S108})$$

10. Processes: $VV \rightarrow f\bar{f}$ with $V = Z', \gamma'$

$$\begin{aligned}
\sigma^{VV \rightarrow f\bar{f}}(s) = & \frac{g_2^4 N_c}{9\pi m_V^4 s(s-4m_V^2) \cos^4 \theta_w} \left\{ \frac{\sqrt{(s-4m_f^2)(s-4m_V^2)}}{m_V^4 + m_f^2(s-4m_V^2)} \right. \\
& \times \left(c_A^4 [-2m_V^8 + m_f^2 m_V^4 (s+4m_V^2) + 2m_f^4 (8m_V^4 - 8m_V^2 s + s^2)] \right. \\
& + 2c_A^2 c_V^2 m_V^4 [8m_f^4 - 6m_V^4 + m_f^2 (22m_V^2 - 7s)] \\
& - m_V^4 (4m_f^4 + 2m_V^4 + m_f^2 s) c_V^4 \Big) \\
& + \frac{\log C}{(s-2m_V^2)} \left(c_A^4 [4m_f^4 (4m_V^2 - s)s + m_V^4 (4m_V^4 + s^2) \right. \\
& + 4m_f^2 m_V^2 (-4m_V^4 - 3m_V^2 s + s^2)] + 2c_A^2 m_V^2 [16m_f^4 m_V^2 \\
& + 3m_V^2 (s^2 + 4m_V^4) + 2m_f^2 (s^2 - 10m_V^2 s - 10m_V^4)] c_V^2 \\
& \left. \left. + m_V^4 [s^2 + 4m_f^2 (s-2m_V^2) - 8m_f^4 + 4m_V^4] c_V^4 \right) \right\}, \tag{S109}
\end{aligned}$$

where

$$C = \frac{s - 2m_V^2 + \sqrt{(s-4m_V^2)(s-4m_f^2)}}{s - 2m_V^2 - \sqrt{(s-4m_V^2)(s-4m_f^2)}}, \tag{S110}$$

and $c_A = a'_f$, $c_V = v'_f$ for $V = Z'$ and $c_A = a''_f$, $c_V = v''_f$ for $V = \gamma'$.

11. Process: $VV \rightarrow \nu\bar{\nu}$ with $V = Z', \gamma'$

$$\begin{aligned}
\sigma^{VV \rightarrow \nu\bar{\nu}}(s) = & \frac{g_2^4 \delta_1^4}{6\pi s} \tan^4 \theta_w \left[\frac{s^2 + 4m_V^4}{(s-4m_V^2)(s-2m_V^2)} \log D - 2 \left(1 - \frac{4m_V^2}{s} \right)^{-1/2} \right] \\
& \times \begin{cases} \epsilon_z^8, & \text{for } V = Z' \\ (\delta_2 - \sin \beta)^4 \epsilon_{\gamma'}^8, & \text{for } V = \gamma' \end{cases}, \tag{S111}
\end{aligned}$$

where

$$D = \frac{s - 2m_V^2 + \sqrt{s(s-4m_V^2)}}{s - 2m_V^2 - \sqrt{s(s-4m_V^2)}}. \tag{S112}$$

12. Processes $f\bar{f}, \nu, \bar{\nu} \rightarrow VV$ with $V = Z', \gamma'$

$$9(s-4m_V^2) \sigma^{VV \rightarrow f\bar{f}} = 8(s-4m_f^2) \sigma^{f\bar{f} \rightarrow VV}, \tag{S113}$$

$$9(s-4m_V^2) \sigma^{VV \rightarrow \nu\bar{\nu}} = 2s \sigma^{\nu\bar{\nu} \rightarrow VV}. \tag{S114}$$

13. Process: $f\bar{f} \rightarrow Z'$

$$\begin{aligned}
\sigma^{f\bar{f} \rightarrow Z'}(s) = & \frac{\pi g_2^2 \delta_1^2 m_{Z'}^2}{2s \sqrt{s-4m_f^2} N_c} \left[\left(1 + \frac{2m_f^2}{m_{Z'}^2} \right) \left(Q_f + \frac{m_{Z'}^2}{2m_W^2} (T_{3f} - 2Q_f) \right)^2 \sin^2 2\theta_w \right. \\
& \left. + \left(1 - \frac{4m_f^2}{m_{Z'}^2} \right) \epsilon_z^4 T_{3f}^2 \tan^2 \theta_w \right] \delta(\sqrt{s} - m_{Z'}). \tag{S115}
\end{aligned}$$

14. Process: $\nu\bar{\nu} \rightarrow Z'$

$$\sigma^{\nu\bar{\nu} \rightarrow Z'}(s) = \frac{3\pi g_2^2 \delta_1^2 \epsilon_z^4 m_{Z'}^2}{s^{3/2}} \tan^2 \theta_w \delta(\sqrt{s} - m_{Z'}). \tag{S116}$$

15. Process: $f\bar{f}, \nu\bar{\nu} \rightarrow \gamma'$

$$\sigma^{f\bar{f} \rightarrow \gamma'}(s) = (\delta_2 - \sin \beta)^2 \sigma^{f\bar{f} \rightarrow Z'}(s) \Big|_{m_{Z'} \longleftrightarrow m_{\gamma'}}. \quad (\text{S117})$$

Same applies to $\sigma^{\nu\bar{\nu} \rightarrow \gamma'}(s)$.

16. Process: $Z' \rightarrow f\bar{f}, \nu\bar{\nu}$

The decay width of Z' to SM fermions is given by

$$\begin{aligned} \Gamma_{Z' \rightarrow f\bar{f}} = & \frac{g_2^2 \delta_1^2 N_c}{12\pi} m_{Z'} \sqrt{1 - \left(\frac{2m_f}{m_{Z'}}\right)^2} \left[\left(1 - \frac{4m_f^2}{m_{Z'}^2}\right) T_{3f}^2 \epsilon_z^4 \tan^2 \theta_w \right. \\ & \left. + \left(1 + \frac{2m_f^2}{m_{Z'}^2}\right) \left(Q_f + \frac{m_{Z'}^2}{2m_W^2} (T_{3f} - 2Q_f)\right)^2 \sin^2 2\theta_w \right], \end{aligned} \quad (\text{S118})$$

and its invisible decay is

$$\Gamma_{Z' \rightarrow \nu\bar{\nu}} = \frac{g_2^2 \delta_1^2 \epsilon_z^4}{8\pi} m_{Z'} \tan^2 \theta_w. \quad (\text{S119})$$